Precambrian Research 422 (2025) 107784

Contents lists available at ScienceDirect

Precambrian Research

journal homepage: www.elsevier.com/locate/precamres

Evidence for a Proterozoic carbonatite system in the Mount Isa Province, Australia

Alex Brown [a,*], Carl Spandler [a,b], Thomas G. Blenkinsop [c]

[a] Economic Geology Research Centre (EGRU) and Geoscience Department, James Cook University, Townsville 4011 QLD, Australia
[b] Department of Earth Sciences, University of Adelaide, Adelaide, SA 5005, Australia
[c] School of Earth and Environmental Sciences, Cardiff University, Cardiff CF10 3AT Wales, UK

ARTICLE INFO

Keywords:
Carbonatite
Mount Isa
Geochronology
Zircon geochemistry

ABSTRACT

Carbonatites are indicators of mantle processes, and they are economically important because of their association with rare earth element (REE), niobium and base metal deposits. Carbonatites and their associated lithologies (i.e. the carbonatite system) have not previously been identified in eastern Australia. We describe veins of dolomite calcite carbonatite, fenites and antiskarn, glimmerite, and alkali pegmatite from the Tommy Creek Domain, of the Eastern Subprovince of the Mount Isa Province (NW Queensland), that constitute a carbonatite system. The system can be identified from field relationships, geochronology, zircon trace elements, and stable and radiogenic isotopes. The emplacement of the carbonatite system coincided temporarily and spatially with regional hydrothermal alteration at ca. 1650 Ma in the Eastern Subprovince, which also has mantle isotopic affinities and is located above the boundary between thin and thick continental lithosphere.

1. Introduction

Carbonatites are a diverse category of silica poor magmatic rocks primarily composed of carbonate minerals. Although only a minor component of the crust, carbonatites are of considerable interest as indicators of mantle processes (e.g. Ashwal et al., 2016; Bell & Simonetti, 2010; Bell & Tilton, 2001; Burke et al., 2003, 2008), and their economic importance is increasing due to their association with rare earth element (REE), niobium and base metal deposits (e.g. Simandl & Paradis, 2018).

Classifications of carbonatites have largely involved descriptive systems based on mineralogy (Mitchell, 2005; Mitchell & Gittins, 2022) or composition (Le Maitre et al., 2002; Woolley & Kempe, 1989), although a more recent genetic based alternative (Yaxley et al., 2022) has been proposed. Yaxley et al. (2022) also advocate for a broader view of the 'carbonatite system', to include not only the carbonate rich igneous rocks, but also the associated metasomatic rocks, melts, fluids and their interaction products.

The foundation of the carbonatite system is the CO_2 rich carbonatite melt, which is thought to be derived from unmixing of low degree partial melting of enriched mantle (Schmidt et al., 2024), although partial melting of crustal carbonate has been shown to be feasible under certain conditions (Durand et al., 2015; Lee et al., 2000) and likely in some carbonatite occurrences (Özkan et al., 2021; Schumann et al., 2019). Carbonatite systems can be emplaced in a variety of geologic settings such as orogenic belts, mantle plumes and large igneous provinces (Humphreys-Williams & Zahirovic, 2021), but the majority of known occurrences are in extensional cratonic and cratonic margin environments (Bailey, 1974, 1977; Simandl & Paradis, 2018; Woolley & Bailey, 2012). Differentiation of carbonatitic melts through the production of carbonate-rich cumulates, can lead to diverse lithologies, fluids (hydrothermal and carbothermal) and metasomatism via interactions with the surrounding host, often over short spatial scales (Mitchell, 2005; Yaxley et al., 2022). Indeed, the degree of disequilibrium between the carbonatite system and host rocks can lead to significant modification of both during and after emplacement, which contributes to some of the deficiencies of purely compositional classifications (Yaxley et al., 2022), as well as potential difficulties in field identification.

Carbonatites are yet to be recognized in the geological record of eastern Australia, despite its long and complicated tectonic history, which includes multiple episodes of extensional tectonics. This may in part be due to poor preservation and the relatively small volumes of typical carbonatite systems, but also to difficulties of recognition in the field, particularly in strongly deformed and altered terranes where they can be easily confused with rocks originating as carbonate sediments or

* Corresponding author.
E-mail address: alexander.brown@my.jcu.edu.au (A. Brown).

https://doi.org/10.1016/j.precamres.2025.107784
Received 23 October 2024; Received in revised form 23 March 2025; Accepted 23 March 2025
Available online 1 April 2025

from hydrothermal processes.

In this paper we describe rocks from the Tommy Creek Domain (TCD) of the Proterozoic Mount Isa Province of north west Queensland, Australia which are interpreted on the basis of field relationships and textures, zircon geochronology and chemistry, and radiogenic and stable isotopes, to be components of a previously unrecognized carbonatite system. This observation has implications for the geodynamic evolution of the Mount Isa Province, as well as providing support for a mantle-derived mass flux contributing to regional scale alteration systems and base metal and REE metallogeny.

1.1. Regional geology

The Mount Isa Province, located in northwestern Queensland and the Northern Territory of Australia (Fig. 1A) is a sequence of sedimentary, bimodal volcanic, and intrusive igneous rocks (Blake, 1987) that have undergone polyphase metamorphism and deformation, possibly in a backarc extensional, upper plate setting (Betts et al., 2006, 2011; Gibson et al., 2018). It is also an important metallogenic province, with significant historic and current reserves of copper, gold, lead, zinc, silver and uranium across a multitude of mineralisation styles including IOCG, sediment hosted copper, shale hosted/Sedex Pb-Zn-Ag and Broken Hill Type Ag-Pb-Zn (Geological Survey of Queensland, 2011).

The geological framework of the Mount Isa Province and its major zones has been summarised and redefined numerous times by previous workers (Betts et al., 2006; Blake, 1987; Blake and Stewart, 1992; Foster and Austin, 2008; Jell, 2013; Southgate et al., 2000). These frameworks divide the province into north–south trending tectonic domains (Western Succession/Fold Belt, Kalkadoon-Leichardt Belt and Eastern Succession/Fold Belt), and propose stratigraphic divisions (Fig. 1A). Two stratigraphic divisions are used in the literature; the Cover Sequence terminology initiated by (Blake, 1987), and the more detailed Superbasin nomenclature derived from the Western Subprovince (Southgate et al., 2000). Stratigraphy and magmatic phases are separated into the superbasin nomenclature of Southgate et al. (2000), and are well summarised as time–space plots by Betts et al. (2011).

The Mount Isa Province features four main groups of felsic magmatism occurring between 1820 Ma and 1480 Ma (Wyborn et al., 1988). These are characterized as dominantly anorogenic I to A type granites, with those intruded at ca. 1500 Ma having granodiorite I type affinities (Wyborn, 1998). Mafic rocks are dominantly basaltic with continental tholeiite compositions (Ellis & Wyborn, 1984), although Gibson et al. (2018) suggest a trend towards more MORB like affinities in the ca. 1655 Ma Toole Creek Volcanics. No references to alkaline magmatism or carbonatites within the Mount Isa Province literature have been identified, except a brief mention of a lamprophyre dyke (Derrick, 1980).

Regionally, metamorphism is dominated by high-temperature, low to medium-pressure greenschist to upper amphibolite facies assemblages, with metamorphic evolution along an anticlockwise P-T-t path (Foster & Rubenach, 2006; Hand et al., 2002). The thermal peak is understood to have occurred at around 1590–1575 Ma (Abu Sharib and Sanislav, 2013; Hand et al., 2002; Pourteau et al., 2018; Rubenach et al., 2008); however this does not coincide with any regionally significant magmatism. There are numerous postulated models for producing this anomalous geothermal gradient, including compression of previously extended continental crust (Etheridge et al., 1987; Oliver et al., 1991); mantle delamination (Loosveld & Etheridge, 1990); heat advection via intrusions due to high mantle heat flow (Rubenach, 1992; Rubenach &

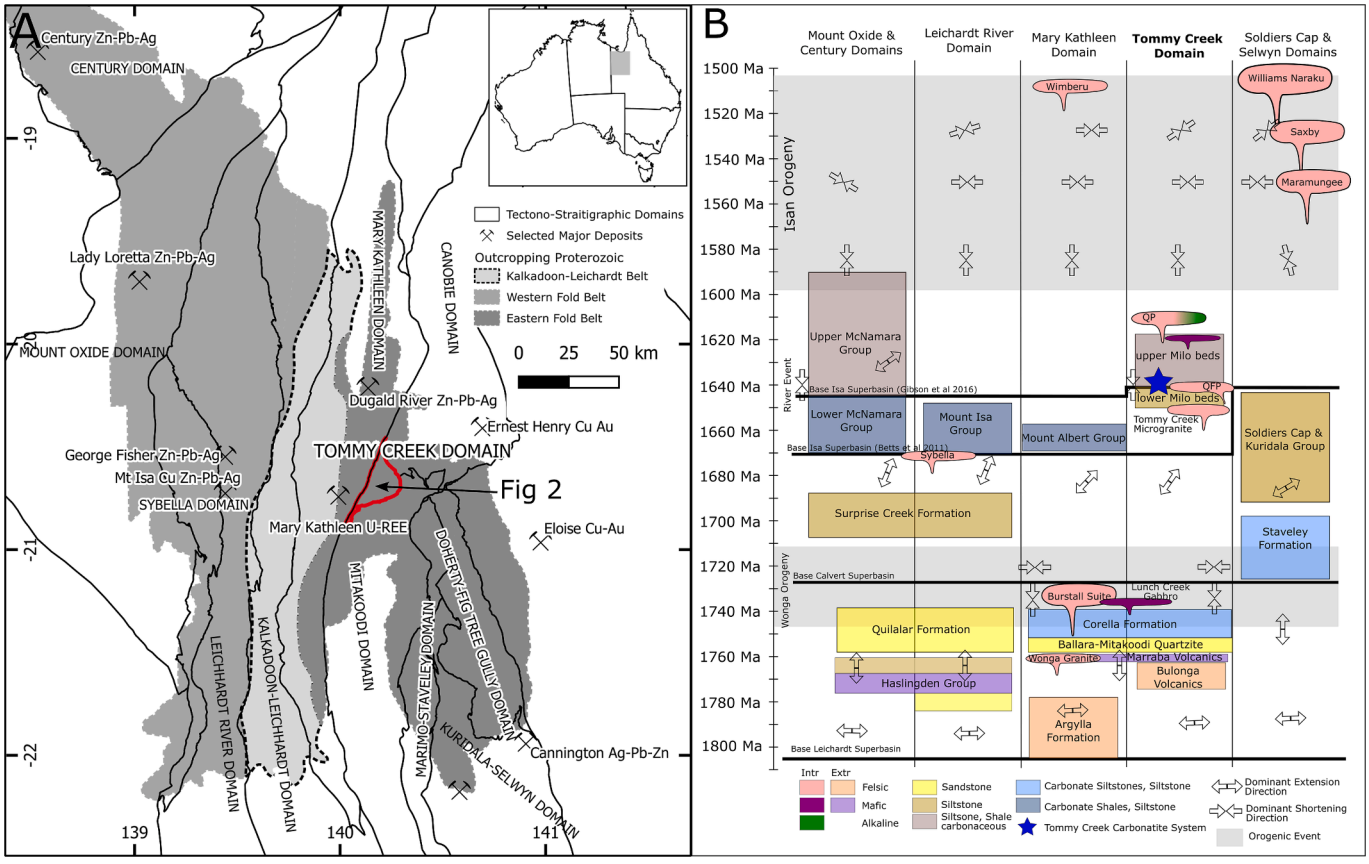

Fig. 1. A) Overview of the Mount Isa Province. Outcropping Proterozoic basement is shaded, and divided into the three main tectonic divisions. The more discrete tectonostratigraphic domains of Betts (et al. 2011) are also shown, along with significant current or historic mining operations. The Tommy Creek Domain, towards the centre of the Province, is highlighted in red. B) A simplified time–space plot for the Mount Isa Province with focus on the Tommy Creek Domain, and major aspects of sedimentation cycles and periods of deformation. The carbonatites of this study are marked in blue. Modified from Brown et al., 2023.

Barker, 1998; Sandiford et al., 1995); radiogenic heating due to enrichment of heat-producing elements in the upper crust (McLaren et al., 1999; Sandiford et al., 1998); and the burial of heat-producing stratigraphic sequences (Hand et al., 2002).

Tectonic syntheses put forward in the literature describe multiple phases of basin development, inversion and orogeny. Three cycles of dominantly east–west extensional rifting and sediment deposition are represented in the superbasin stratigraphic framework. This rifting is punctuated by periods of sedimentary hiatus or basin inversion, and extensive intrusive magmatism (e.g. Burstall suite, Sybella Batholith) (Betts et al., 2006, 2011; Blake, 1987; Foster & Austin, 2008; Loosveld, 1989; Southgate et al., 2000).

The Isan Orogeny commenced ca. 1600 Ma and continued through to ca. 1500 Ma (Betts et al., 2006), halting the superbasin development. This was the dominant period of deformation and metamorphism, and can be broadly broken into four main stages) (Betts et al., 2011).

The geodynamic setting of basin formation has been more contentious. Early work suggested an intracratonic setting (Carter et al., 1961), then a continental margin (Wilson, 1978), whereas (Blake, (1987) and Loosveld (1989) proposed an intracontinental rifting model. A far-field margin influence forming a backarc basin was proposed the early-mid 2000 s (Betts et al., 2006; Giles et al., 2002) and is currently a favoured interpretation (eg. Gibson et al., 2018).

The TCD is a fault bounded package of calc-silicate, metasedimentary and metavolcanic rocks with felsic and mafic intrusions, and a complex and intense deformation history. The metamorphic grade is anomalously high relative to neighbouring domains, being dominated by amphibolite facies rather than the greenschist facies of adjacent blocks (Blake, 1987; Foster & Rubenach, 2006; Hill et al., 1992; Lally, 1997). A chronostratigraphic framework for the TCD is presented by Brown et al. (2023), and regional scale time–space plot with focus on the TCD and the rocks described in this paper is presented in Fig. 1B. Metasedimentary rocks can be split into two main groups: calc-silicate, marble and fine-grained clastic rocks equivalent to the Corella Formation (ca. 1760–1720 Ma), and younger volcanic rocks, siliciclastic rocks, marl and black shale of the Milo beds (ca. 1660–1620 Ma). These units host a suite of felsic, mafic and alkaline rocks with ages of 1640 Ma and 1620–1610 Ma (Brown et al., 2023). Intrusions of this age do not feature prominently elsewhere in the Mount Isa Province.

1.2. Study area geology

The study area has been described by Brown et al., (2023), which is summarized here. Covering approximately 13 km^2 in the central portion of the TCD, the area comprises a complexly folded exposure of the Milo beds juxtaposed against the surrounding Corella Formation across a similarly complex deformation zone (Fig. 2). The Corella Formation is dominated by granoblastic calc-silicate rocks with variable proportions of amphibole (actinolite, hornblende), diopside, feldspar (albite and orthoclase), calcite and quartz, as well as calcareous metasiltstones and lenses of coarse-grained calcitic marble, commonly with metamorphic calc-amphiboles and pyroxenes.

The Milo Beds can be separated into an upper and lower sequence, with the lower sequence comprising feldspathic psammites and volcano-sedimentary rocks with lenses of medium to coarse grained dolomitic marble. The marble commonly has diopside and actinolite grains to 10 mm, and minor biotite and chlorite to 1 mm. Internal bedding of marble layers is generally not clear, although layer parallel fabric defined by dark minerals or boudinaged shale interlayers is commonly observed. The volcano-sedimentary rocks, which include ribbon breccias and probable relict fiamme, correlate to the Tommy Creek Beds of Hill et al. (1992). The upper sequence comprises biotite metasiltstones, muscovite schist, graphitic phyllite (generally 5–15 % total graphitic carbon) and biotite-garnet schist. The graphitic phyllite locally contains andalusite, staurolite and sillimanite. The age of the Milo beds is constrained by maximum depositional ages (from detrital zircons) of ca. 1660 Ma (lower sequence) and ca. 1640 Ma (upper sequence), and minimum depositional age of ca. 1620 Ma based on the age of cross-cutting intrusions (Brown et al., 2023).

This metasedimentary package is intruded by a multitude of felsic, mafic and alkaline igneous rocks, of which only the Tommy Creek Microgranite (1650 Ma, Anderson et al., 2017) has been named (Fig. 2). It is a pink two feldspar equigranular granitic rock with grainsize 1–5 mm, and accessory hornblende or biotite. This unit is predominantly found to the northeast of the study area in a doubly plunging sill complex intruding the Corella Formation.

Several porphyritic phases of rhyodacitic composition have been identified, including feldspar phyric (QFP), quartz phyric (QP) and biotite ocelli bearing (QFB). These form sills and stocks that intrude both the Corella Formation and Milo beds. Zircon geochronology has shown these formed in two different events, with the QFP sills emplaced ca. 1640 Ma and remainder between 1620 and 1610 Ma (Brown et al., 2023).

Two main mafic phases have been identified in the study area. The most prominent is a composite sill composed of gabbro and pyroxenite, metamorphosed to a coarse grained amphibolite and a magnesian chlorite-pyroxene-amphibole schist respectively, both being locally garnet bearing. Relict olivine has been observed in the chlorite schist. A small mafic dyke cutting the gabbro constrains the minimum age to 1618 ± 10 Ma. The second phase is a fine to medium grained biotite bearing dolerite to trachyte. Both are found as dykes or sills primarily in the upper Milo Beds, with the true thickness of the metagabbro-pyroxenite likely exceeding 100 m.

The study area hosts a series of cryptic alkaline intrusive phases that are subtle and difficult to identify and distinguish in the field from their hosts, and are the focus of this study. These include syenitic pegmatite and glimmerite that have only been identified in drill core as narrow veins with apparent thicknesses of up to 10 m, as well as a series of carbonate-rich veins, up to 30 m apparent thickness, that intrude both the Milo beds and the QFP units. As we show later in this work, these carbonate-rich rocks belong to a carbonatite system. Therefore, for simplicity, we describe them hereafter as carbonatites.

There are a number of base metal and REE ± fluorite mineral occurrences and exploration prospects in, and within 5 km of, the study area, including Milo (overlapping Cu-Au and REE mineralisation), Beacon (fluorite-U-REE), Brownsnake (adjacent REE and Cu-Au) and Tommy Creek (Cu-Au ± Zn)(Fig. 2). None of these are currently considered economic, although a mineral resource is reported for Milo of 88 Mt at 0.11 % Cu and 176 Mt at 620 ppm total rare earth and yttrium oxide (GBM Resources, 2012).

Deformation at the map scale is apparent as an early E-W fold refolded by a N-S fold (Figs. 2, 3). Strong foliations and crenulation cleavages developed in micaceous lithologies of the upper Milo Beds, and the rhyodacite porphyries exhibit strong linear fabrics. Metamorphic assemblages, particularly the sillimanite in the graphitic phyllite, point towards peak thermal conditions of > 500 °C, consistent with the findings of Foster & Rubenach, (2006).

2. Methods

Data collected in this study are available in the linked data repository.

2.1. Zircon U-Pb geochronology and trace elements

Samples were prepared and analysed for U-Pb geochronology alongside those reported in Brown et al. (2023). Trace element data were collected by LA-ICPMS from 22 samples previously used for geochronology, primarily to investigate the possibility of discriminating different zircon origins. Spot analyses were performed using a Teledyne Analyte G2 193 nm ArF excimer laser ablation system and a Thermo iCAP-TQ quadrupole mass spectrometer at the Advanced Analytical

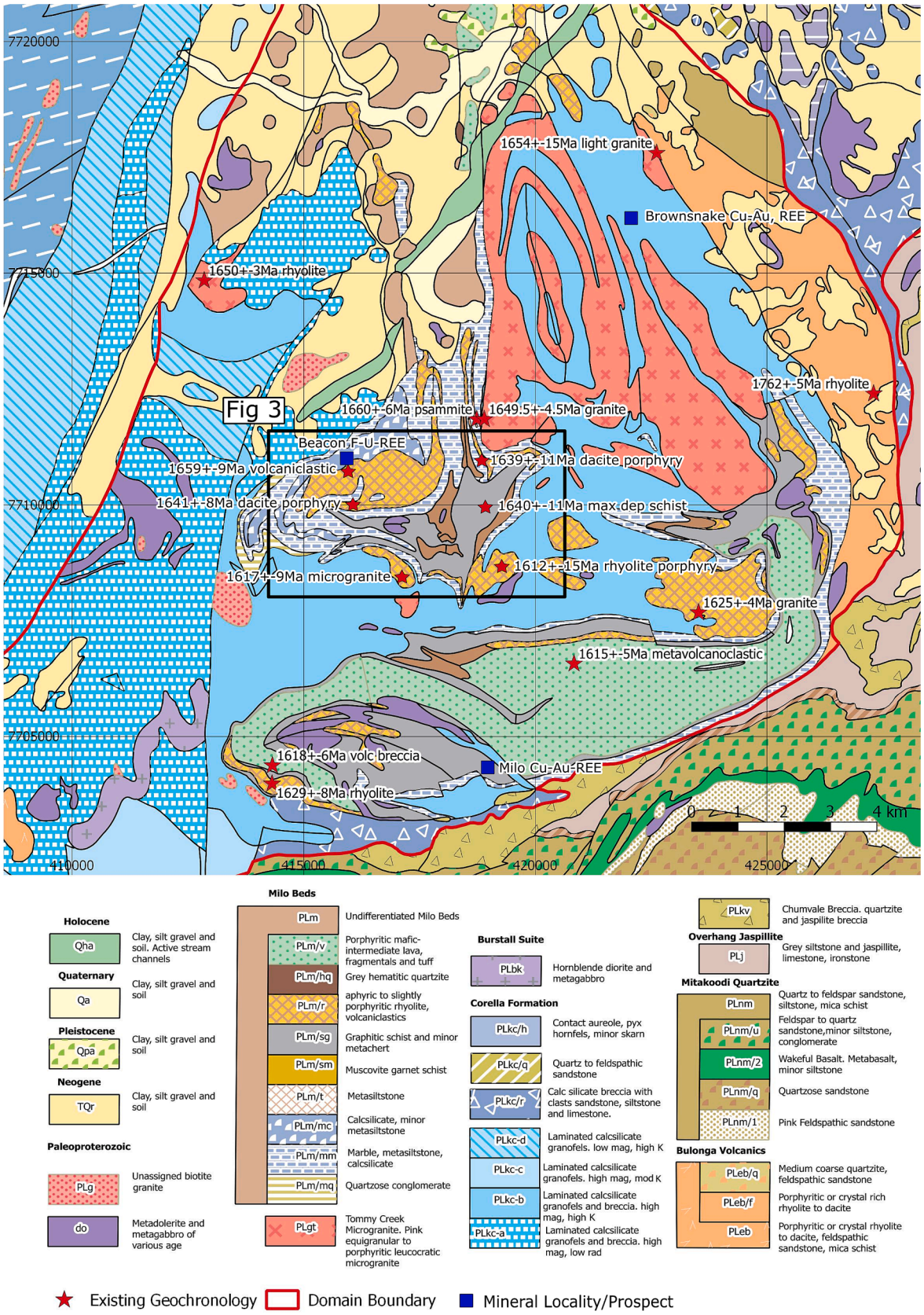

Fig. 2. Geology of the central Tommy Creek Domain according to data released with the Northwest Queensland Mineral and Energy Province Report (Geological Survey of Queensland, 2011; Geological Survey of Queensland et al., 2015). Geochronology sites are shown with the age and sample lithology(Anderson et al., 2017; Brown et al., 2023), and mineral localities/deposits of interest are marked in blue.

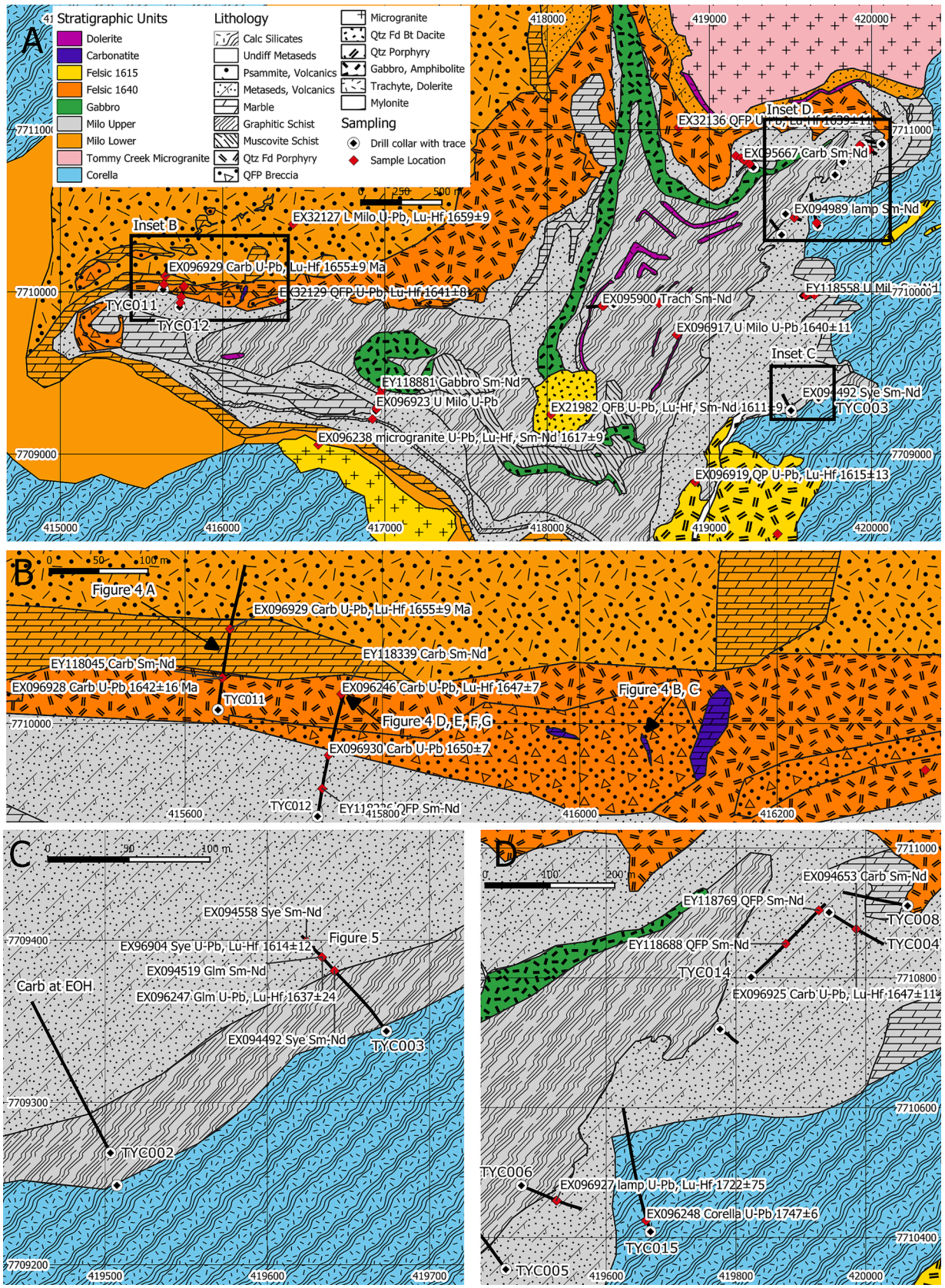

Fig. 3. Map of the study area in the central Tommy Creek Domain, including sample locations presented in this study. Grid coordinates Australian Geodetic Datum 1984 Zone 54. Most samples are drill core and therefore do not necessarily correlate with the mapped surface geology. Insets B-D show areas of particular interest where carbonatite and associated lithologies were intersected in drilling or surface outcrops were located. Labels take the form of: sample ID rock type method age. EOH = end of hole.

Centre (AAC) at James Cook University, Townsville. Ablation was performed at 5 Hz and 2.5–3 J/cm^2, with spot sizes of 20–30 μm. Between 15 and 30 analyses were taken for each sample, with the following masses collected: ^{27}Al, ^{29}Si, ^{31}P, ^{43}Ca, ^{45}Sc, ^{49}Ti, ^{55}Mn, ^{57}Fe, ^{88}Sr, ^{89}Y, ^{91}Zr, ^{93}Nb, ^{139}La, ^{140}Ce, ^{141}Pr, ^{143}Nd, ^{147}Sm, ^{151}Eu, ^{157}Gd, ^{159}Tb, ^{163}Dy, ^{165}Ho, ^{167}Er, ^{169}Tm, ^{171}Yb, ^{175}Lu, ^{178}Hf, ^{181}Ta, ^{204}Pb, ^{206}Pb, ^{232}Th, ^{238}U. Data was reduced in iolite (Paton et al., 2011) using both Si and Zr as internal standards, although in general the Si dataset was used. For zircon trace elements, NIST610 glass (Jochum et al., 2011) was used as an external standard, with GJ1, FC1 and Temora used as check standard. Results were inspected using ioGAS.

2.2. Whole rock geochemistry and stable isotopes

The whole rock dataset is a series of commercial four acid and fusion digests with atomic emission spectroscopy (AES) or mass spectrometry (MS) from the mineral exploration dataset of drill core and rock chip samples collected by MIM Resource Development Pty Limited (MIMRD) as part of a Cu-Au mineral exploration program. Sample preparation and analysis was performed by ALS Global, with methods ME-ICP61, ME-MS61, ME-ICP06, ME-MS81 (trace and major elements), Au-AA21 (gold), C-IR07 (total carbon), C-IR18 (graphitic carbon) variably employed across the dataset. Stable C and O isotopes in carbonate from bulk rock powders for 44 samples from 9 different lithologies were determined using ALS method LS-ISTP01, which is a Laser Spectroscopy method performed by the Mineral Deposit Research Unit, University of British Columbia. Samples and analyses were collected by MIMRD over a period between 2014 and 2022. QAQC was monitored using commercially available OREAS standards inserted at an average rate of 1 per 50 samples, in addition to the run standards used by ALS (average 1 in 20 samples). This data, as well as the associated drillhole and other metadata can be found online via the Geological Survey of Queensland Open Data Portal at the following references: Brown, 2017, 2018, 2019. Although the quality of analyses of these datasets is high, it must be noted that the samples were collected for the purpose of mineral exploration at scale and as such sampling was conducted over 1 to 2 m intervals and not necessarily respecting small scale heterogeneities, particularly in unmineralised country rock, which can potentially limit their applicability to detailed geochemical characterisation of rock types.

2.3. Whole rock Sm-Nd isotopes

A total of 25 Sm-Nd isotope determinations were made on archival laboratory pulps from previously assayed drill core and rock chip samples from 9 different lithologies. Sm-Nd isotope analyses were performed in two campaigns at the University of Adelaide following the routine described in Meeuw et al. (2019). Between 50 and 200 mg of the samples were digested in PARR acid (HNO_3-HF acid mix) digestion bombs at 190 °C for 96 h, then evaporated to dryness and bombed with 6 M HCl overnight. The samples were spiked with a ^{150}Nd-^{147}Sm spike and then separated by column chromatography. Isotopic abundance and ratios were then determined with a Phoenix Isotopx thermal ionisation mass spectrometer (TIMS). The measurements were corrected for mass fractionation by normalisation to ^{146}Nd/^{144}Nd = 0.7219. The Nd reference material JNdi-1a was processed and yielded an average ^{143}Nd/^{144}Nd value for respective sessions of 0.512103 ± 0.000014 and 0.512103 ± 0.000008 (2sd, n = 5 and 5, standard reference value = 0.512115 ± 0.000007 (Tanaka et al., 2000)), whereas the USGS rock standard G-2 returned a ^{143}Nd/^{144}Nd value of 0.512205 ± 0.000019 and 0.512223 ± 0.000012 (2sd, n = 2 and 3, reference value 0.512233 ± 0.00001; GeoReM preferred value). Measurements were used to calculate εNd, as well as CHUR and Depleted Mantle Model ages using the values of Goldstein et al. (1984). For the age of formation, most samples can be related directly to U-Pb geochronology samples. Others were assigned an age using the geochronological framework of the Tommy Creek area (Brown et al., 2023).

3. Results

3.1. Field and petrographic description of alkaline intrusive phases

3.1.1. Carbonatites

Carbonatites are primarily recognized in drill core as narrow veins with apparent thicknesses in the order of 10 cm to 30 m, and are rarely recognized in surface mapping (Fig. 3). These rocks are composed of 0.5–2 mm grains of calcite, dolomite and phlogopite. The carbonates are commonly clear and vitreous, giving the rock an overall 'sugary' appearance. At hand specimen scale, other minerals with more variable abundance include diopside and tremolite or actinolite.

Intrusive relationships can be positively identified in both surface exposures and drill core. An example of carbonatite at location 20.7076S 140.1945E (Fig. 3B, Fig. 4B,C) is a vein cutting through brecciated QFP and can be correlated to QFP identified in drill core collared nearby. At surface, the carbonatite is a dark grey to black micaceous sugary textured rock (Fig. 4C). The most striking field relationships have been identified in drillcore, where carbonatites can be seen crosscutting the QFP unit, forming brecciated margins and hosting QFP xenoliths with prominent phlogopite reaction rims (Fig. 4D,F,G). Where hosted by metasiltstones, alteration selvedges comprising alkali feldspar −carbonate −tremolite ± diopside ± chlorite are commonly observed (Fig. 4A).

In thin section the rock is dominated by clean, crystalline calcite and dolomite with generally evenly dispersed phlogopite grains in an interlocking texture. Diopside and magnesian actinolite or tremolite are minor minerals. Accessory phases include zircon (particularly visible due to pleochroic halos in the phologpite in reaction rims and throughout the rock), apatite, rutile, titanite and sulfides such as pyrite, chalcopyrite and sphalerite. Rare phases such as baryte, REE and Nb silicates and oxides were identified using energy dispersive spectroscopy (EDS) while observing thin sections on a Hitachi SU5000 SEM (Fig. 5).

3.1.2. Syenitic pegmatites

No surface expression of the syenitic pegmatite dykes have been found, although coarse silicified material in the expected surface locations may represent leached and weathered versions. In drill core, intervals of 5 to 30 m apparent thickness have been identified. The rock comprises coarse to very coarse (1–5 cm) grains of K-feldspar and blue green Na-Ca amphibole, with lesser phlogopite and minor titanite with similar grain size (Fig. 6D, E). Late veins of quartz ± pyrite ± carbonate are present, but in general the rock is quartz absent. Thin sections reveal that plagioclase and microcline are both present, with some indications of hypersolvus textures. Accessory minerals include zircon, chlorite, rutile likely as an alteration of titanite, and fluorite associated with phlogopite as inclusions along cleavage planes (Fig. 6F).

3.1.3. Glimmerite

The glimmerite is observed as 0.5 to 3 m apparent thickness veins cutting metasedimentary rocks with irregular contacts. The rock is composed of > 70 % black coarse phlogopite with a roughly equant, interlocking grains with no preferred orientation (Fig. 6 A, B). Grains of K-feldspar up to 10 mm are a minor phase, and interstitial ankerite, pyrite and fluorite are visible at hand specimen scale (Fig. 6B). In thin section, a most striking feature is the abundance of fluorite, most commonly as cleavage filling inclusions and replacements within the phlogopite, and only rarely as veinlets or space infill (Fig. 6C). The phlogopite is often ragged in appearance and show distorted cleavage traces. The main accessory phase identified is zircon.

3.2. Geochronology

Zircon U-Pb geochronology is a potential tool to help discriminate

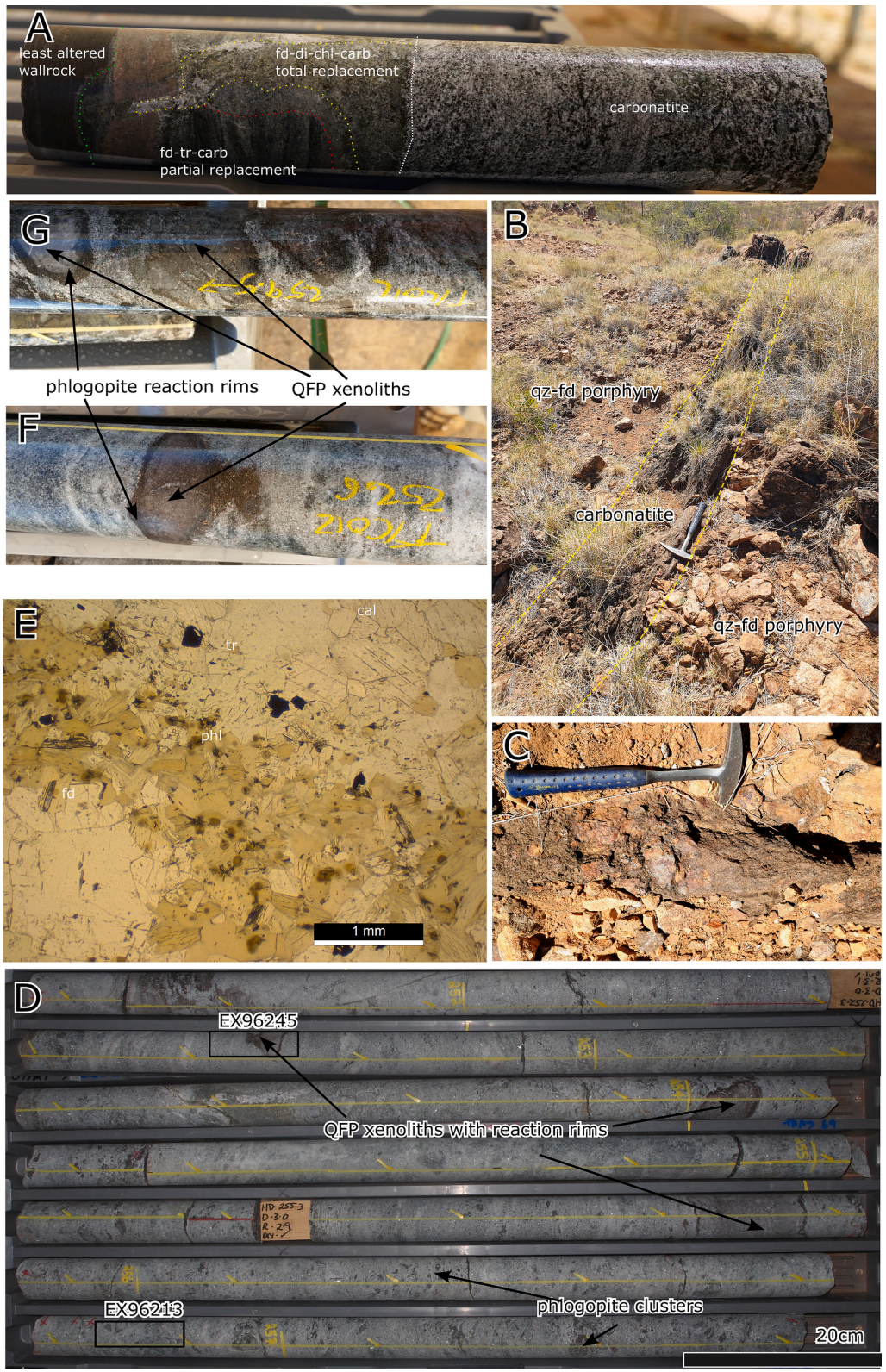

Fig. 4. A)Drill core (TYC011) showing contact zone between carbonatite and metasedimentary wall rocks. Various degrees of replacement alteration of the wall rock by carbonate, chlorite, sericite, tremolite, diopside and titanite are visible. B and C) examples of narrow dyke of intrusive carbonate cutting through the quartz-feldspar porphyry QFP unit. D) Drill core (TYC012) showing some of the features and textures of the carbonatite, including xenoliths of wall rock with phlogopite reaction rims and smaller clusters of phlogopite. Locations corresponding to samples shown in Fig. 5 are also marked E) PPL optical photomicrograph of carbonatite (top right) with QFP clast (lower left) and phologopite-tremolite reaction rim (diagonal). Sample EX096245. F and G) drill core (TYC012) showing clasts of QFP with phlogopite reaction rims from the margins of intrusive carbonate dyke. Pink tinge to clast in F is due to fine titanite alteration of the clast. Sample locations in Fig. 3.

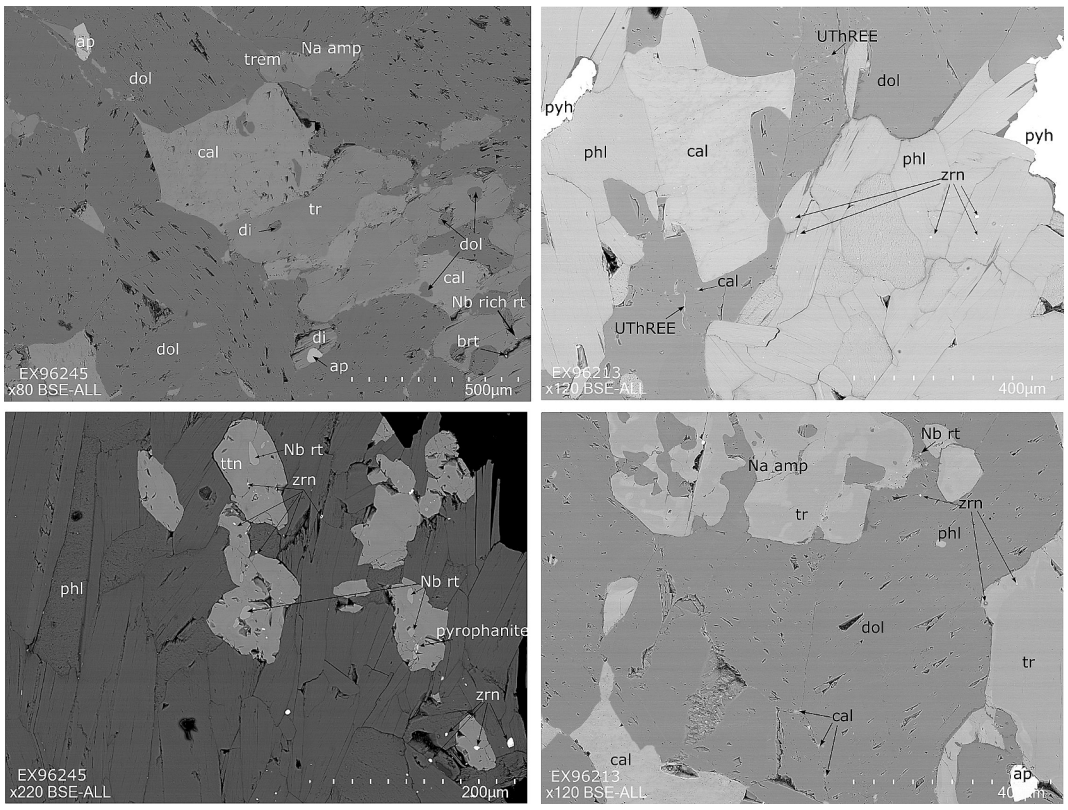

Fig. 5. SEM photomicrographs of polished sections of carbonatite showing an assemblage of dolomite (dol), calcite (cal) and phlogopite (phl) with minor tremolite (tr), Na rich amphibole (Na amp) and diopside (di). Accessory phases include apatite (ap),zircon (zrn), titanite (ttn), Nb rich rutile (rt), baryte (brt), pyrophanite, pyrrhotite (pyh) and unidentified U, Th and LREE minerals.

intrusive versus sedimentary origins of the carbonate units, with sedimentary carbonates more likely to yield a spectrum of ages due to detrital input, if any zircon can be extracted at all. Some samples had strong field indicators of their origin, such as veins through the QFP unit with xenoliths (carbonatite) or interbedded with siltstone and shale (marbles). All carbonate rocks have low whole-rock Zr values (50–80 ppm); nonetheless, samples identified as carbonatite were productive for zircons in mineral separation. The marbles were not as productive, with most samples yielding insufficient zircons to generate a useable dataset. Two marble samples yielded adequate zircons and produced detrital populations with ages ~ 1650 Ma, ~1725 Ma and 1850–2700 Ma (Brown et al, 2023). Results of the zircon geochronology for the carbonatite samples are presented in Table 1, along with key samples reported in Brown et al. (2023). In general, the carbonatite samples produced robust, single age populations, and had a higher proportion of concordant results compared to most other samples from the study area. The determined ages for all five samples are within error of each other at ca. 1647 Ma. This age is also within error of the ages obtained from the QFP unit (Brown et al. 2023), which many of these samples intrude or contain xenoliths thereof, and as such the possibility of zircon inheritance was investigated via zircon trace element chemistry.

3.3. Zircon trace elements

Trace element data for zircon from the study area used for geochronology presented here and in Brown et al. (2023) were examined to evaluate potential differences in zircon origin. Results are presented in Fig. 7, and data aggregated by sample can be found in the supplementary material.

Some key observations from the data include; 1) the low values for REE and HFSE in carbonatite-hosted compared to felsic-hosted samples; 2) very high REE, and HFSE in pegmatite sample EX21980; 3) Th/U ratios are generally > 0.5 for all samples; 4) the chemistries of zircons hosted by the carbonatite and QFP are quite distinct and do not support inheritance; 5) the trace elements are low in general, consistent with other carbonatite zircons (e.g. Belousova et al., 2002; Nedosekova et al., 2016; Tshiningayamwe et al., 2022).

3.4. Isotopic results

Two different isotopic systems, carbonate C-O and whole rock Sm-Nd, were used to potentially discriminate between the carbonate units and to gain petrogenetic insights into the nature of various units within the study area.

3.4.1. Whole rock Sm-Nd isotopes

Complete whole rock Sm-Nd isotope data can be found in the supplementary material, and results aggregated by lithology are shown in Table 2 and Fig. 8. Some key observations from the data include; 1) εNd (i) values between + 1.4 and + 2.6 suggest a primitive signature for the mafic rocks, in particular the gabbro-pyroxenite (εNd(i) = +2.6) 2) The two main felsic phases, QFP (1642 Ma, εNd(i) = -3.39) and QP (1610–1615 Ma, εNd(i) = -0.69) are distinct from one another, suggesting different sources, with the younger felsic phase (QP) having a more primitive source and; 3) The carbonatites and Milo beds marbles have overlapping εNd(i) of ~ -3.

3.4.2. Carbon and oxygen stable isotopes

Carbonate carbon and oxygen stable isotope data are presented in Fig. 9 and in the supplementary material. Key observations from the data include; 1) all lithologies show distinct signatures compared to unaltered sedimentary carbonate; 2) the results are along trends previously observed with widespread Na-Ca alteration in the Eastern Subprovince (Marshall et al., 2006; Oliver et al., 1993); 3) there is no

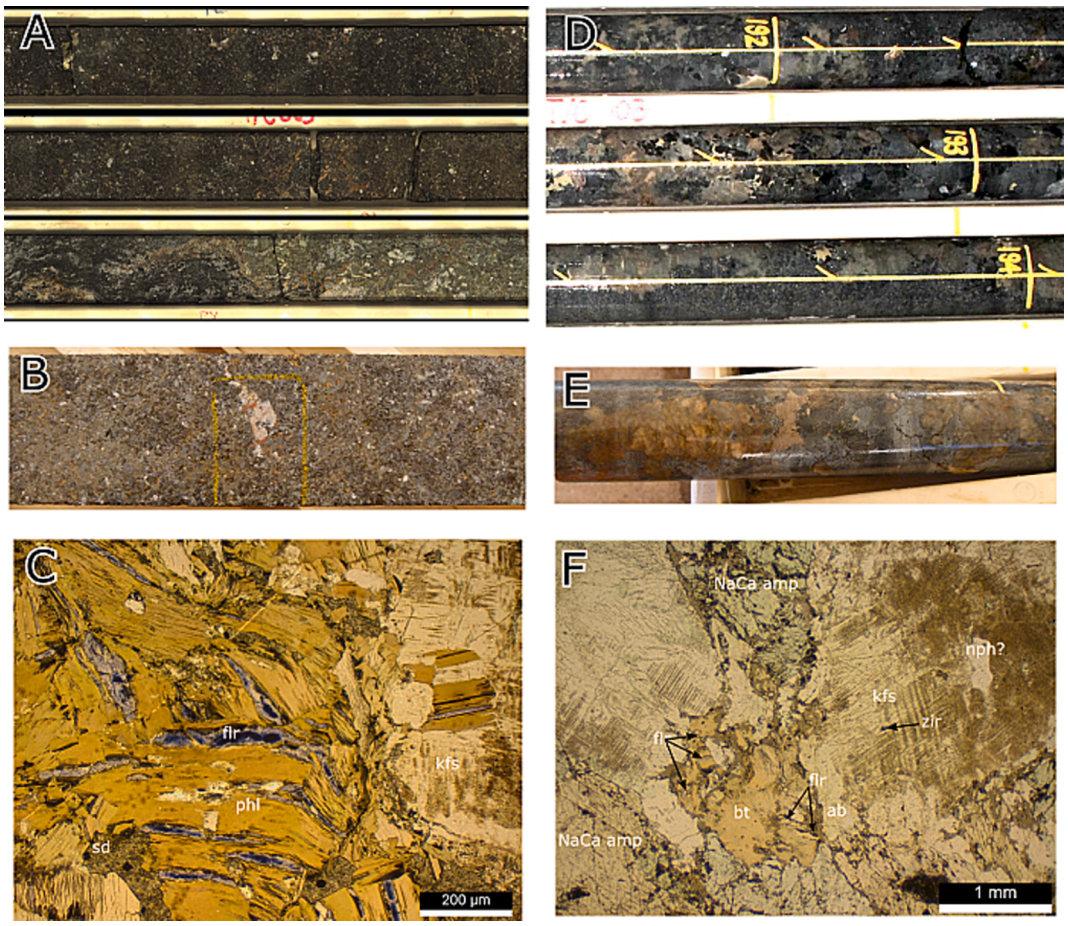

Fig. 6. A) drill core showing massive coarse phlogopite from a glimmerite dyke. B) massive coarse phlogopite with phenocrysts of K-feldspar and minor siderite infill. C) Plane-polarized light optical photomicrograph from glimmerite showing coarse biotite-phlogopite and K-feldspar and accessory siderite. Fluorite is comonly seen exploiting cleavage surfaces of phlogopite, but not as crosscutting veins. D and E) syenitic pegmatite with coarse K-feldspar, blue green Na-Ca amphibole and minor titanite and phlogopite. F) Plane-polarized light optical photomicrograph of syenitic pegmatite with microcline and albite, Na-Ca amphibole and biotite with accessory fluorite and zircon. All photos are from samples from drill hole TYC003, A, B and C 166–171 m; D&E 190–210 m; F 136 m.

Table 1
Zircon U-Pb ages from this study, along with selected samples from Brown et al. 2023.

Sample	Lithology	Unit	Spots	Age 1	Age 2	Comment
EX096901	Fine-grained mafic within coarse mafic.	Gabbro	19	1618 ± 10		Brown et al. 2023
EX096246	Carbonate-biotite rock with QFP xenoliths	Carbonatite	65, 35	1647 ± 7 (n = 76)		
EX096925	Carbonate-biotite-pyroxene	Carbonatite	63 [48]	1647 ± 11 (n = 48)		48 concordant
EX096928	Carbonate- biotite	Carbonatite	27	1642 ± 16 (n = 22)		
EX096929	Carbonate- biotite	Carbonatite	49	1655 ± 10 (n = 38)		38 concordant
EX096930	Carbonate- biotite with xenoliths	Carbonatite	26	1645 ± 9 (n = 9)		Reverse discordance
EX96904	very coarse pegmatitic syenite. Amph-fd-bt-tit. Some late qtz	Syenite pegmatite	36, 53	1616 ± 21 (n = 11)	1725 ± 15 (n = 29)	Very scattered data, possible common Pb. Also 1822 ± 22 Ma (n = 16). Brown et al. 2023
EX096247	coarse phlogopite- K feldspar	Glimmerite	32	1616 ± 20 (n = 11)	1657 ± 18 (n = 8)	Scattered data making difficult to interpret. Brown et al. 2023

systematic discrimination possible between lithologies based on C and O isotopes alone.

No samples lie within the mantle isotopic field (e.g. the ocean basalt field used by Bell & Simonetti, 2010), however the data from the study area is consistent with the spread of isotopic values for carbonatites worldwide (Bolonin, 2019).

3.5. Lithogeochemistry

Major element analyses from mineral exploration drill core assays are presented in Fig. 10, and are consistent with typical values of CaO (20–30 %), MgO (12–18 %) and Fe_2O_3 (5–10 %) for magnesiocarbonatite using the scheme of Le Maitre et al. (2002). A trend toward ferrocarbonatite is apparent, but is better explained as the influence of overprinting pyrite, pyrrhotite and chalcopyrite mineralisation, with a

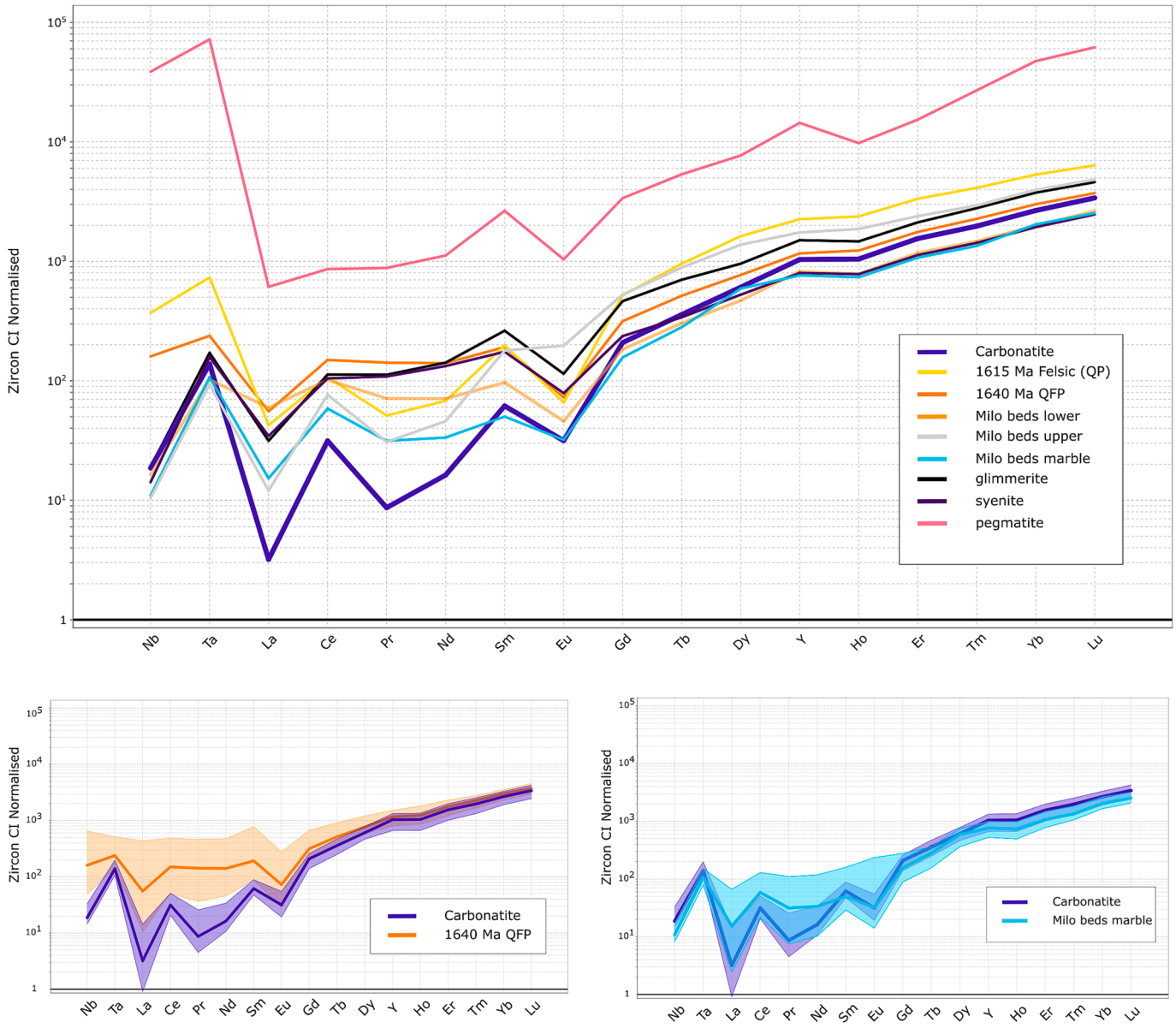

Fig. 7. Zircon trace elements normalised to chondrite (McDonough & Sun, 1995). (A) analyses grouped by unit and showing median value. Note relative depletion of HFSE and LREE in intrusive carbonate (B) comparison of data from carbonatite and QFP (line = median, field = 25th to 75th percentile) showing distinct compositions that are unlikely to be the same population despite very similar ages (C) comparison of data from carbonatite and Milo beds marble (line = median, field = 25th to 75th percentile). There is overlap partly due to the wider variability of the marble samples, reflecting the detrital nature of the zircons.

Table 2
Whole rock Sm-Nd results aggregated by lithology.

	Count	Age (Ma)	εNd Mean	εNd stdev	TDM (Ma)	TCHUR (Ma)
Glimmerite	1	1615	−1.40		2422	1809
Milo Beds: marble	4	1630	−3.75	0.72	2468	2018
carbonatite	4	1645	−2.84	0.56	2480	1976
Dolerite	2	1620	1.41	0.49	1973	1499
Gabbro	3	1625	2.61	0.64	2050	1226
QFP	4	1641	−3.39	0.20	2317	1928
QP	4	1615	−0.69	0.69	2180	1688
Syenite pegmatite	2	1615	−3.62	0.11	2766	2192

strong correlation increasing Fe with sulfur evident. SiO_2 (10–30 %) and Al_2O_3 (0.5–5 %) are variable and consistent with carbonatite compositions, although they likely reflect significant interaction and contamination with the country rock. The syenite and glimmerite are both magnesium (8–13 % MgO) and alkali rich (6–12 % $Na_2O + K_2O$) suggesting the presence of phlogopite in the glimmerite, and alkali rich amphiboles in the syenite in addition to feldspar.

The trace element dataset is more ambiguous, with the samples only having only modest concentrations of carbonatite-indicator elements such as Ba, Nb, Sr and REE (Simandl & Paradis, 2018). There is considerable trace element composition overlap between samples labelled as carbonatite and marble. This could be attributed to significant geochemical interaction between carbonatite and country rock (see Discussion), but also likely reflects some degree of data smearing given the large interval of sampling used for this mineral exploration dataset.

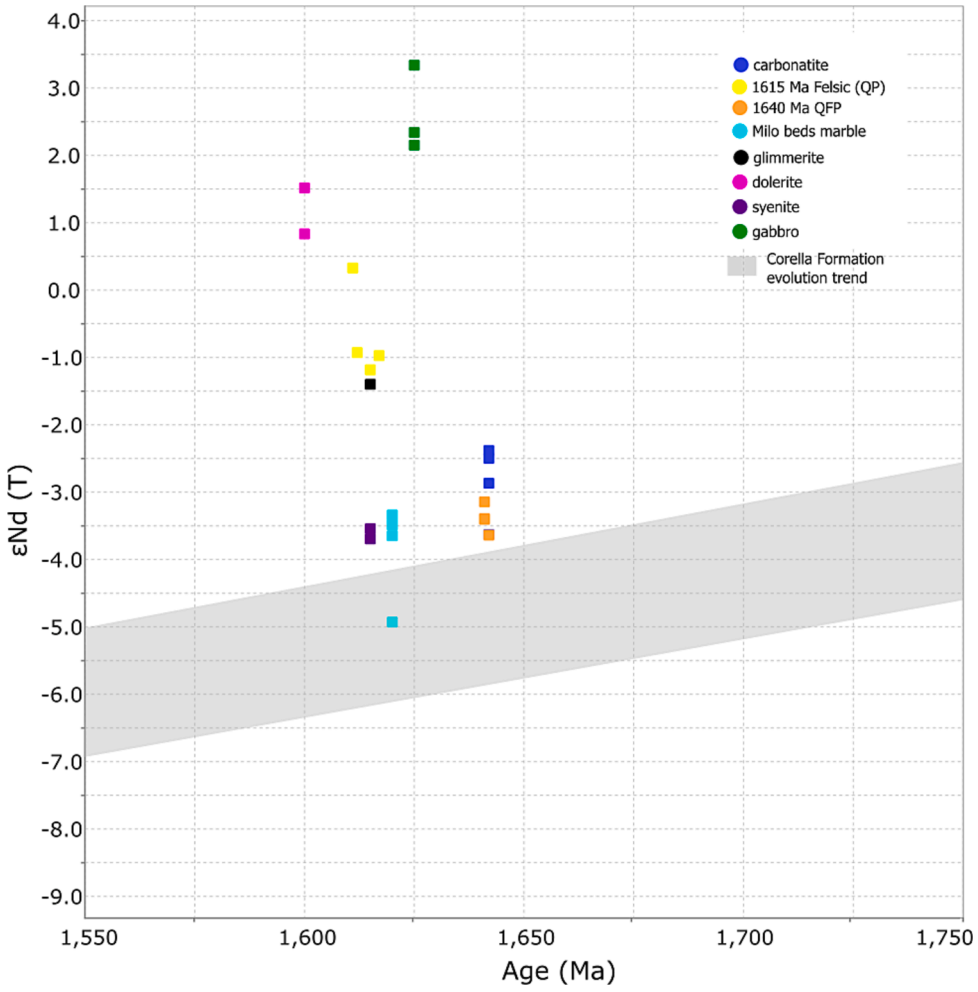

Fig. 8. Plot of εNd(t) vs age for samples collected in this study and compared to the evolution trend of the Corella Formation metasedimentary rocks from Maas et al., 1987.

4. Discussion

4.0.1. Evidence for a carbonatite system

Discrimination of carbonatites from other carbonate bearing units can often be difficult, particularly if they do not form large magmatic complexes such at Phalaborwa (South Africa), those of the Kola Alkaline Province (Russia), or those of the East African Rift Zone (Bell & Blenkinsop, 1987; Tichomirowa et al., 2006; Yuhara et al., 2005). This is further complicated in terranes with complex deformation, metamorphism and metasomatic histories (Simandl & Paradis, 2018), such as the Mount Isa Province. In such cases, any single criterion is likely to be inadequate to confidently categorise a given occurrence of carbonate bearing rock. Therefore, the approach taken here is to bring together multiple aspects to build the case for the presence of a carbonatite system (Yaxley et al., 2022) in the study area.

Deformed and brecciated sedimentary carbonates (marbles, dolomites, marls etc.) are a common feature of many formations in the Mount Isa Province, including the Milo beds and Corella Formation found in the study area (Marshall, 2003). Additionally, numerous phases of carbonate (dominantly calcite) veining are present due to extensive hydrothermal events across the Mount Isa Province (Marshall et al., 2006; Oliver et al., 1991, 2008).

In the study area, field relationships such as crosscutting relationships with igneous rocks, the presences of felsic xenoliths (Fig. 4) and proximal wall-rock alteration (e.g. glimmerite, alkali feldspar-carbonate-amphibole-pyroxene selvedges) and brecciation are compelling indicators of the intrusive nature of some carbonates, showing that they are either magmatic or hydrothermal veins. Conversely, some carbonate bodies show clear sedimentary field relationships, such as interbedding with metasiltstone and shale. In other samples from drill core or strongly weathered subcrop, field relationships are not always clear. This ambiguity can also be increased by mobility of carbonate rocks during deformation, which has affected both the carbonatite system rocks and sedimentary carbonates.

The use of zircon geochronology and zircon trace element chemistry is key in unravelling the cryptic carbonate rocks in the study area. Many samples of the carbonatite units produced high zircon yield with a good single population of concordant U-Pb ages all at ~ 1647 Ma (range 1642–1655 Ma). This is very similar to, and within error of the age of, the QFP (~1641 Ma). Field relationships show that the intrusive carbonates postdate the QFP (crosscutting veins, QFP xenoliths, and brecciated margins).

Trace elements in zircon provide further evidence that zircons from carbonatite samples are distinct from the felsic rocks they intrude and from sedimentary carbonate samples. Zircons from the carbonatite samples have distinctly lower LREE compared to the felsic and detrital samples (Fig. 7), and, along with zircons from the other alkaline samples, have lower Ti, Nb, and Ta compared to zircons from the felsic igneous rocks (Fig. 7). These results show that the carbonatite zircons are unlikely to have been inherited from the 1640 Ma QFP, despite their similar ages. Zircons from the Milo beds metasedimentary rocks are also

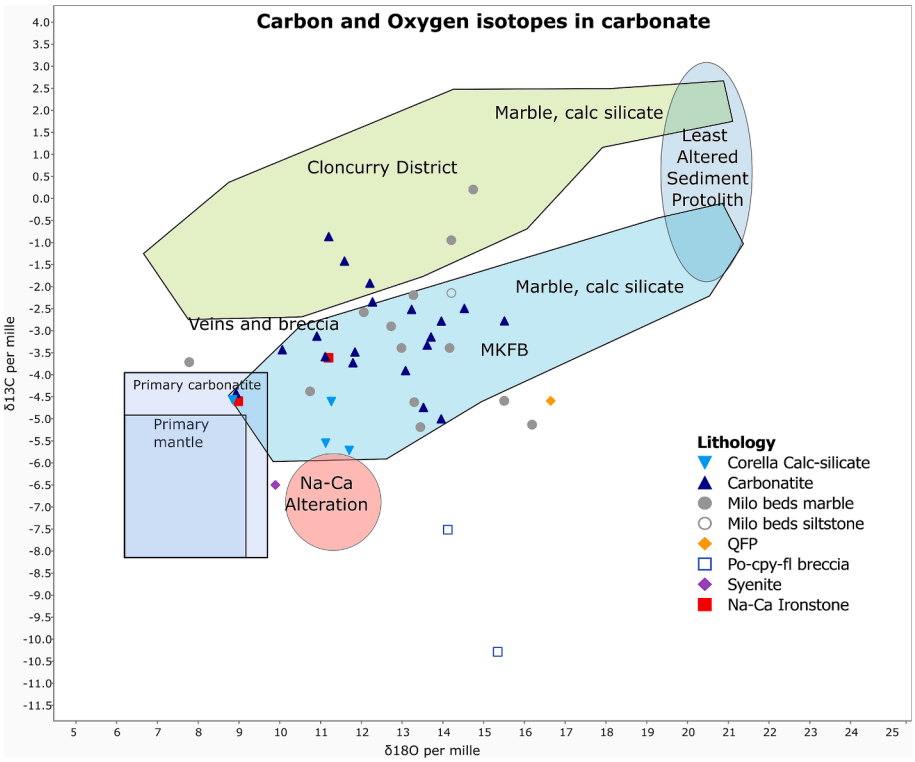

Fig. 9. Plots of carbonate C and O isotope results over fields from marble, calc-silicate, vein and breccias of the Corella Fm from the Cloncurry District and Mary Kathleen Fold Belt (MKFB)(Marshall et al., 2006). There is a strong overlap between carbonatite and marble populations, however neither have the heavier signatures typical of marine carbonates, and are consistent with the regional alteration signature. Primary mantle and carbonatite fields from (Keller & Hoefs, 1995; Taylor et al., 1967).

distinct from the carbonatite, although not to the same degree as the igneous rocks. This pattern of low trace elements in the carbonatitic zircon, particularly P, Ti, Nb and REE, is consistent with other reports of alkaline rock hosted and carbonatite hosted zircons (Belousova et al., 2002; Hoskin & Ireland, 2000; Nedosekova et al., 2016; Tshiningayamwe et al., 2022), and contrasts with hydrothermal zircon which is commonly enriched in these trace elements (Hoskin, 2005). Trace element concentrations and U/Pb ages in zircon are therefore a possible tool to help discriminate the carbonatite from the metasedimentary rocks in this area.

Bulk rock geochemistry and mineralogy of the carbonate units in the study area are variable, and there is no decisive discriminator in the collected dataset. With similar bulk-rock major element and mineral compositions, it would be expected that major post metamorphic mineral assemblages of both carbonatite and marble would be similar, and textural modification (grain size, fabrics etc.) during metamorphism and deformation is also likely to obscure any original differences. Nonetheless, antiskarn style reactions – assimilation of silica into the carbonatite melt from wall rocks producing mineral assemblages similar to skarns (Anenburg & Mavrogenes, 2018) – are a likely explanation for the observed diopside and amphiboles and phlogopite in reaction zones, such as rims around xenoliths of QFP (Fig. 4; Anenburg & Walters, 2024; Slezak et al., 2021), as well as shifting the bulk geochemical and isotopic composition towards that of the country rock. The feldspar-carbonate-amphibole-pyroxene wall rock alteration commonly observed in metasediment wall rock is evidence for either fenitisation or antiskarn formation, both common alteration features of carbonatite systems.

Whilst hydrothermal carbonate veining is widespread and diverse within the Mount Isa Eastern Subprovince, large veins (>1 m thickness) are generally calcitic in composition and very coarse grained (Oliver et al., 2004, 2008). Amphiboles (actinolite and tremolite) and pyroxenes (diopsides) are common, although biotite is not. By contrast, glimmerite is considered a common product of carbonatite wall rock reactions (Anenburg & Walters, 2024; Witt et al., 2019, Williams-Jones et al., 2024). Moreover, the presence of fluorite in the glimmerite (Fig. 5C) is consistent with the common association of fluorite with altered wall rocks to carbonatites (Li et al., 2023; Palmer & Williams-Jones, 1996; Stepanov et al., 2024).

Numerous workers have used various isotopic systems, such as C-O and Sm-Nd to characterize magmatic processes forming carbonatites (e.g. Bell & Blenkinsop, 1987; Bell & Tilton, 2001; Chakhmouradian et al., 2008; Downes et al., 2014; Simonetti et al., 1995; Simonetti & Bell, 1994; Tichomirowa et al., 2006; Tilton et al., 1998; Wen et al., 1987). These generally show mantle-like signatures (positive εNd, negative δ13C, moderate to strongly positive δ18O); however there is significant diversity globally (Bolonin, 2019; Slezak & Spandler, 2020; Yaxley et al., 2022). The carbonatites in this study show Sm-Nd (εNd = -2.4 to −3.6), δ13C (−1 to −6 ‰) and δ18O (9 to 15.5 ‰) values consistent with those reported in the literature, especially those from Precambrian terranes (Yaxley et al., 2022). However, there is not sufficient difference between the intrusive carbonates and marbles to allow decisive discrimination. The C-O isotope signature of the carbonatites in this study could be interpreted to be due to melt reaction with country rock, causing isotope shifts away from primary mantle values. Such interaction with silicate country rocks is also apparent from the silicate phases and reaction products (antiskarn, glimmerite) discussed previously. However, these C-O isotopes values are also not sufficiently different from the isotopic composition of other carbonate bearing rocks in the central TCD and elsewhere in the Eastern Subprovince (Fig. 9) that are attributed to the regional scale Na-Ca alteration events of the Isan Orogeny (1600 – 1490 Ma) (Hingst, 2002; Marshall et al., 2006; Oliver et al., 1993).

Taken together, the weight of evidence suggests that the intrusive carbonates are part of a carbonatite system based on:

- Intrusive field relationships with country rock, including felsic intrusions.

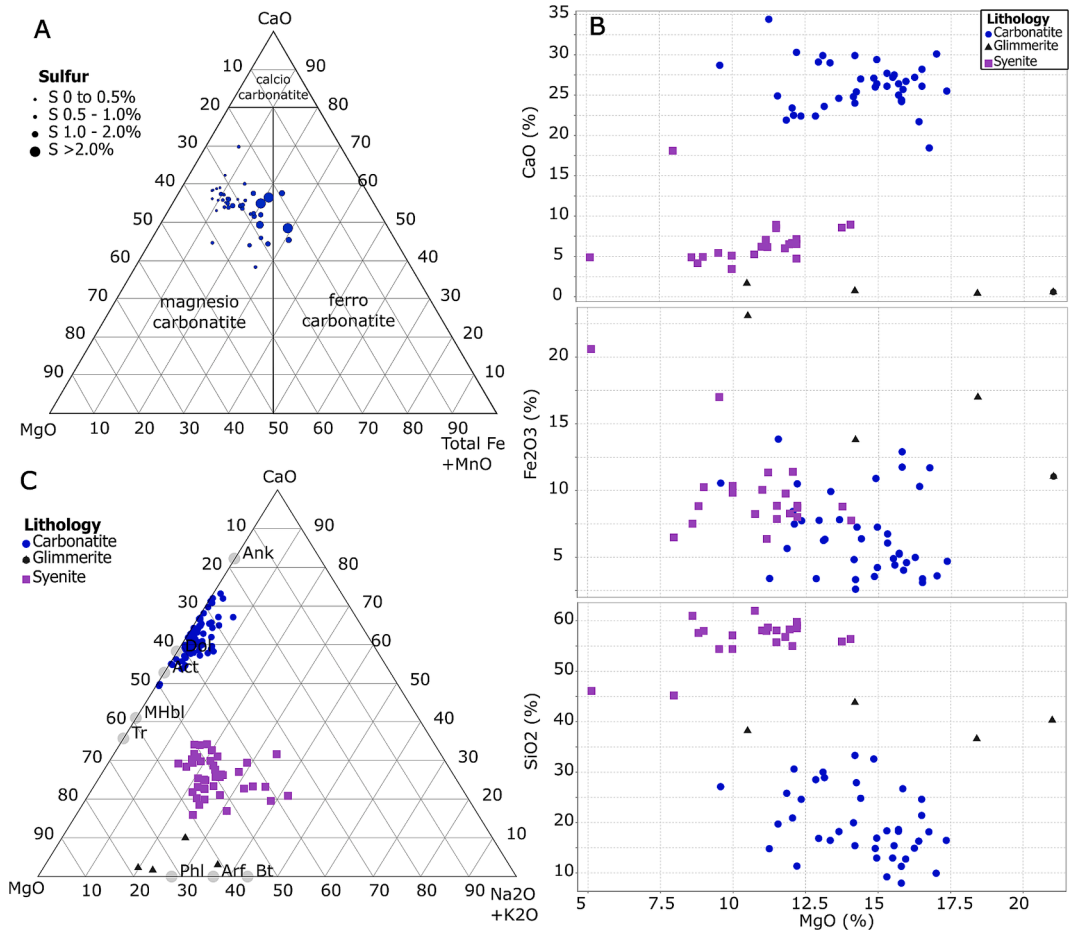

Fig. 10. Major element analysis presented in various diagrams (A) IUGS carbonatite classification ternary, with points sized by sulfur. This shows the carbonatite should be classified as a magnesiocarbonatite in this scheme. A trend towards ferrocarbonatite is visible, however this correlates strongly with sulphur, and is related to pyrite, pyrrhotite and chalcopyrite mineralisation hosted in some of the carbonatite occurrences. (B) Major element plots for CaO, Fe_2O_3 and SiO_2 against MgO. The low values of SiO_2 and very high combined CaO and MgO (primarily carbonate) is consistent with typical carbonatite composition. The syenite and glimmerite are also MgO rich. (C) Ternary diagram with CaO, MgO and Alkali ($Na_2O + K_2O$) axes. The carbonatite population is centred over a dolomitic composition, with trends towards magnesian amphibole and calcite. The glimmerite plots closer to the phlogopite node compared to non end-member biotite. The syenite is quite alkali rich, suggesting that alkali amphiboles (arfvedsonite node plotted) are an important constituent. Mineral nodes Ank = ankerite, Dol = dolomite, Act = Actinolite, MHbl = magnesian hornblende, Tr = tremolite, Phl = phlogopite, Arf = arfvedsonite, Bt = biotite (Fe = Mg).

- Xenoliths of felsic country rock.
- Reaction products/selvedges with silicate wall rocks (fenitisation, antiskarns) consistent with those observed in other carbonatite systems.
- Presence of accessory apatite, Nb silicates and REE phases in the carbonatite dykes, and presence of fluorite in the glimmerite.
- Consistent, single age zircon populations (not detrital).
- Zircon trace element geochemistry that is distinct from other units in the study area, and consistent with other published carbonatite zircons.
- Isotopic (Sm-Nd, C and O) values consistent with a mantle source showing some crustal contamination.
- Presence of other alkali or silica undersaturated rock types (syenite pegmatite, glimmerite) commonly associated with carbonatite systems.
- The occurrences of REE and fluorite-REE-base metal mineralisation, which may be part of a carbonatite system (as defined by Yaxley et al., 2022) that is yet to be fully delineated.

Despite these features, positive identification of carbonatite system rocks in any given location in the study area can be challenging. Complex deformation (modification of contacts and fabrics, boudinage and disruption of stratigraphic units), metamorphism (mineralogy changes) and alteration history (hydrothermal overprints, veining) that are ubiquitous across the Mount Isa Eastern Subprovince obfuscate the possible origins of any given occurrence of carbonate rock. For these reasons, carbonatites may be under-recognised and more widespread within the TCD and the Mount Isa Eastern Subprovince, and indeed in other complex polymetamorphic terranes across the globe.

4.0.2. *Reaction products vs cumulates*

Recent studies have emphasized the diverse rock types and processes involved in carbonatite systems, in particular the importance of reaction derived rocks as distinct from those crystallising directly from melts (Yaxley et al., 2022, Anenburg and Mavrogenes, 2018, Anenburg and Walters, 2024). Carbonatites are commonly considered to be carbonate cumulates (Schmidt et al., 2024), with their chemistry reflecting this differentiation from a mantle sourced melt. The chemistry of reaction dominant components of the carbonatite system however, may be highly variable depending on multiple factors such as country rock composition, melt and derived fluid evolution, and the degree of interaction of the fluid and country rock.

A number of the lines of evidence used above to demonstrate the presence of a carbonatite system in the TCD are also consistent with most of the rock units and features formed as primarily reaction

products rather than cumulate phases. The presence of zircon, generally thought to be inconsistent with primary carbonatite melt compositions (Gervasoni et al., 2017; Li et al., 2024), is a strong indicator of assimilation of silica from the wall rock. This is consistent texturally, with the zircons observed in thin section and on SEM closely related to phlogopite clusters and mantles (Fig. 4E, Fig. 5). This texture, and the consistent morphology, age and chemistry of the zircons makes the main alternative explanation of carbonatite hosted zircon, xenocrysts from along the transport path, seem unlikely.

Aspects of the geochemistry also point to significant country rock interaction, such as SiO_2 and Al_2O_3 composition, the general similarity across the trace elements and stable isotopes between carbonatite and country rock, and lack of strong geochemical indicators such as Ba-Sr and REE (Simandl & Paradis, 2018). It should be noted that we do not interpret the entire carbonatite system in the TCD to be deficient in these components, as mineralisation localities peripheral to the study area with considerable enrichment in REE (Milo, Beacon, Brownsnake) and F-Ba (Beacon) potentially belonging to this carbonatite system.

Finally, the morphology of the observed carbonatite rocks, as widespread narrow veins, would favour melt − country rock interaction and the production and preservation of reaction zones. This may then be further compounded by post emplacement regional scale metasomatic and metamorphic events.

4.0.3. Melt source; mantle versus crustal?

Anatexis of crustal carbonate rocks as a carbonatite melt source has been shown to be plausible at temperatures as low as 600 °C (at 2 kbar) (e.g. Durand et al., 2015; Floess et al., 2015; Wyllie & Tuttle, 1960), and recent studies identify such occurrences in the field (Ferrero et al., 2016; Floess et al., 2015; Liu et al., 2006; Schumann et al., 2019; Wickramasinghe et al., 2024; Wu et al., 2022). These examples have geochemical and isotopic characteristics similar to adjacent metasedimentary rocks, but show textural and field evidence of being igneous in origin. The TCD carbonatites have some geochemical, isotopic, mineralogical and field relation similarities to these examples, however the study area did not reach the high metamorphic grades observed in the other studies (granulite facies), with metamorphic peak, estimated as upper amphibolite (550–600 °C at ca. 1580 to 1600 Ma (Brown et al., 2023; Foster & Rubenach, 2006), occurring some 40 to 70 m.y. after the TCD carbonatites (ca. 1650 Ma). Moreover, the TCD carbonatites were emplaced at very shallow (and hence relatively cool) crustal levels, being contemporaneous with deposition of the host stratigraphy (Brown et al., 2023). Fluorine and other components are known to significantly lower solidus conditions of carbonatites (Jago and Gittins 1991) and we do observe significant fluorite in glimmerite (Fig. 5C), so it is feasible that a F-rich volatile flux into marble may have instigated localized anatexis of the marble. However, such a scenario is inconsistent with the distinctly different age population, geochemistry of zircons from the carbonatites and marbles. Moreover, in this scenario we would also expect to see anatexis of clastic metasedimentary rocks of the sequence, as such a volatile flux would cause a similar lowering of the solidus of these compositions (e.g. Li et al 2022). We have not, however, observed evidence of anatexis of the sedimentary package in the study area. Thus, it seems unlikely that the TCD carbonatites are of anatectic origin, and if they are, melt generation required an F (±alkalis) fluid flux, which would only feasibly come from crystallising alkali magmatism. In this case, carbonatite genesis would still be inextricably linked to mantle processes, given the mantle origin of alkaline magmatism (see below).

4.0.4. Tectonic setting

With crustal anatexis deemed unlikely, we favour a mantle origin for the TCD carbonatite melts. The isotopic signatures reported here for the TCD carbonatites, whilst consistent with the global carbonatite dataset, extends to an origin from more enriched mantle and/or a degree of crustal input through tectonic recycling or assimilation into the original melt. Further modification of these signatures through interaction with the country rock during emplacement would also contribute to the observed data.

Carbonatite systems are generally found in continental lithosphere (with a bias towards craton margins), although the tectonic setting can be variable, including intraplate, rifts, and orogens (Humphreys-Williams & Zahirovic, 2021). A significant change in lithospheric thickness (measured by the depth of the lithosphere-asthenosphere boundary, LAB) occurs below the Mount Isa Province, and has been observed empirically to have an association with sediment-hosted base metal systems in Australia and globally (Hoggard et al., 2020). This LAB topography is also likely to be favourable for the development of a carbonatite system, in particular during discrete geodynamic events such as rifting or orogeny (Humphreys-Williams & Zahirovic, 2021), and is consistent with most current tectonic interpretations of the Mount Isa Province (Betts et al., 2006, 2011; Blenkinsop et al., 2008; Gibson et al., 2018). The identification of a carbonatite system in the Mount Isa Province highlights the importance of the LAB transition as a first order control on the tectonic, hydrothermal and metallogenic evolution of the region.

4.0.5. Relationship to regional alteration and metallogenesis

The Eastern Subprovince has extensive volumes of metasomatised rock, including widespread Na-Ca alteration, and more localized IOCG related alteration and mineralisation (Oliver et al., 2004, 2008). The bulk of the hydrothermal activity is attributed to the Isan Orogeny. However, an earlier Na-Ca (1670–1630 Ma) event is described in the Soldiers Cap Group, which is of similar age to the TCD carbonatites (Foster & Austin, 2008; Rubenach et al., 2008). The origin of CO_2 in the Na-Ca regional alteration is attributed to an enriched mantle source on the basis of the isotopic signature (Oliver et al., 2008).

Thus, the carbonatite system in the TCD coincides in time and space with widespread significant fluxes of mantle derived fluids that contributed to extensive hydrothermal alteration, and brecciation in the Eastern Subprovince at ca. 1650 Ma. These processes may have led directly to mineralisation (e.g. precursors to REE occurrences, metal flux into the upper crust in hydrothermal and magmatic fluids) as well as preparing the Subprovince for subsequent ore formation in the Isan orogeny via the creation of mechanically favorable or reactive hosts for IOCG deposits, and fertilisation of mid-crustal melt source regions (Oliver et al. 2008).

5. Conclusion

Intrusive carbonate (carbonatite) and associated alteration (fenitisation, antiskarn) and alkali rich rocks (glimmerite, syenite), along with REE and fluorite-REE mineral occurrences are proposed to be components of a carbonatite system in the TCD of the Mount Isa Eastern Subprovince. Field relationships, mineralogy, textures, geochemistry, geochronology, and radiogenic and stable isotopic signatures are all consistent with a carbonatite origin, and signify the first reported occurrence of carbonatite in the Mount Isa Province, and eastern Australia. The carbonatite system coincided temporally (at ca 1650 Ma) and spatially (in the Eastern Subprovince) with regional hydrothermal alteration linked to base metal and REE mineralisation, and to a flux of carbon-bearing fluids with mantle isotopic signatures, suggesting a significant transfer of mass and energy from the mantle into the crust. The carbonatite system overlies a step in the lithosphere-asthenosphere boundary in the Mount Isa Province, providing further evidence of the importance of these boundaries in localizing dynamic mantle-crust interactions.

CRediT authorship contribution statement

Alex Brown: Writing – original draft, Visualization, Investigation, Formal analysis, Conceptualization. **Carl Spandler:** Writing – review & editing, Supervision. **Thomas G. Blenkinsop:** Writing – review & editing, Supervision, Investigation.

Funding

Funding and support for this work was provided by Mount Isa Mines, whom A Brown was employed by for the duration of the project.

Declaration of competing interest

The authors declare the following financial interests/personal relationships which may be considered as potential competing interests: [Alex Brown reports financial support and administrative support were provided by Mount Isa Mines. If there are other authors, they declare that they have no known competing financial interests or personal relationships that could have appeared to influence the work reported in this paper].

Acknowledgements

The authors thank the technical assistance from James Cook University colleagues Yi Hu and Shane Askew of the Advanced Analytical Centre as well as Huiqing Huang. Valuable feedback on the manuscript from anonymous reviewers is very much appreciated. Mount Isa Mines is thanked for funding and project support.

Appendix A. Supplementary data

Supplementary data to this article can be found online at https://doi.org/10.1016/j.precamres.2025.107784.

Data availability

Data supporting the findings of this paper can be accessed at James Cook University at https://doi.org/10.25903/q81t-7t34

References

Abu Sharib, A.S.A.A., Sanislav, I.V., 2013. Polymetamorphism accompanied switching in horizontal shortening during Isan Orogeny: example from the Eastern Fold Belt, Mount Isa Inlier, Australia. Tectonophysics 587, 146–167. https://doi.org/10.1016/j.tecto.2012.06.051.

Anderson, J. R., Fraser, G. L., McLennan, S. M., & Lewis, C. J. (2017). A U–Pb geochronology compilation for northern Australia: Version 1, November 2017.

Anenburg, M., Mavrogenes, J.A., 2018. Carbonatitic versus hydrothermal origin for fluorapatite REE-Th deposits: experimental study of REE transport and crustal "antiskarn" metasomatism. Am. J. Sci. 318 (3), 335–366. https://doi.org/10.2475/03.2018.03.

Anenburg, M., Walters, J.B., 2024. Metasomatic ijolite, glimmerite, silicocarbonatite, and antiskarn formation: Carbonatite and silicate phase equilibria in the system Na2O–CaO–K2O–FeO–MgO–Al2O3–SiO2–H2O–O2–CO2. Contrib. Miner. Petrol. 179 (5), 40. https://doi.org/10.1007/s00410-024-02109-0.

Ashwal, L.D., Patzelt, M., Schmitz, M.D., Burke, K., 2016. Isotopic evidence for a lithospheric origin of alkaline rocks and carbonatites: an example from southern Africa. Can. J. Earth Sci. 53 (11), 1216–1226. https://doi.org/10.1139/cjes-2015-0145.

Bailey, D.K., 1974. Continental rifting and alkaline magmatism. In: Sorensen, H. (Ed.), The Alkaline Rocks. Wiley, pp. 148–159.

Bailey, D.K., 1977. Lithosphere control of continental rift magmatism. J. Geol. Soc. London 133 (1), 103–106. https://doi.org/10.1144/gsjgs.133.1.0103.

Bell, K., Blenkinsop, J., 1987. Nd and Sr isotopic compositions of East African carbonatites: implications for mantle heterogeneity. Geology 15 (2), 99–102. https://doi.org/10.1130/0091-7613(1987)15<99:NASICO>2.0.CO;2.

Bell, K., Simonetti, A., 2010. Source of parental melts to carbonatites–critical isotopic constraints. Mineral. Petrol. 98 (1), 77–89. https://doi.org/10.1007/s00710-009-0059-0.

Bell, K., Tilton, G.R., 2001. Nd, Pb and Sr isotopic compositions of east african carbonatites: evidence for mantle mixing and plume inhomogeneity. J. Petrol. 42 (10), 1927–1945. https://doi.org/10.1093/petrology/42.10.1927.

Belousova, E.A., Griffin, W.L., O'Reilly, S.Y., Fisher, N.I., 2002. Igneous zircon: trace element composition as an indicator of source rock type. Contributions to Mineralogy and Petrology; Heidelberg 143 (5), 602–622. https://doi.org/10.1007/s00410-002-0364-7.

Betts, P. G., Armit, R. J., Hutton, L., J., Withnall, I. W., & Donchak, P. J. T. (2011). Mount Isa Inlier Geodynamic Synthesis. In Geological Survey Queensland, North West Queensland Mineral and Energy Province Report. Department of Employment, Economic Development and Innovation.

Betts, P.G., Giles, D., Mark, G., Lister, G.S., Goleby, B.R., Aillères, L., 2006. Synthesis of the proterozoic evolution of the Mt Isa Inlier. Aust. J. Earth Sci. 53 (1), 187–211. https://doi.org/10.1080/08120090500434625.

Blake, D.H., 1987. Geology of the Mount Isa Inlier and environs. Queensland and Northern Territory. Australian Govt. Pub. Service.

Blake, D.H., Stewart, A.J., 1992. Detailed studies of the Mount Isa inlier. Australian Govt. Pub. Service.

Blenkinsop, T.G., Huddlestone-Holmes, C.R., Foster, D.R.W., Edmiston, M.A., Lepong, P., Mark, G., Austin, J.R., Murphy, F.C., Ford, A., Rubenach, M.J., 2008. The crustal scale architecture of the Eastern Succession, Mount Isa: the influence of inversion. Precambr. Res. 163 (1), 31–49. https://doi.org/10.1016/j.precamres.2007.08.011.

Bolonin, A.V., 2019. Oxygen and carbon isotope composition in primary carbonatites of the world: data summary and linear trends. Open Journal of Geology 9 (8). https://doi.org/10.4236/ojg.2019.98028.

Brown, A. (2017). EPM 12561, FOUNTAIN RANGE, ANNUAL REPORT FOR PERIOD ENDING 9/8/2017—GSQ Open Data Portal. https://geoscience.data.qld.gov.au/data/report/cr102697.

Brown, A. (2018). EPM 12561, FOUNTAIN RANGE, ANNUAL REPORT FOR PERIOD ENDING 9/8/2018—GSQ Open Data Portal. https://geoscience.data.qld.gov.au/data/report/cr108461.

Brown, A. (2019). EPM 12561, FOUNTAIN RANGE, ANNUAL REPORT FOR PERIOD ENDING 9/8/2019—GSQ Open Data Portal. https://geoscience.data.qld.gov.au/data/report/cr114432.

Brown, A., Spandler, C., Blenkinsop, T.G., 2023. New age constraints for the Tommy Creek Domain of the Mount Isa Inlier. Australia. Australian Journal of Earth Sciences 70 (3), 358–374. https://doi.org/10.1080/08120099.2023.2171124.

Burke, K., Ashwal, L.D., Webb, S.J., 2003. New way to map old sutures using deformed alkaline rocks and carbonatites. Geology 31 (5), 391–394. https://doi.org/10.1130/0091-7613(2003)031<0391:NWTMOS>2.0.CO;2.

Burke, K., Khan, S., Mart, R., 2008. Grenville Province and Monteregian carbonatite and nepheline syenite distribution related to rifting, collision, and plume passage. Geology 36, 983–986. https://doi.org/10.1130/G25247A.1.

Carter, E. K. (Edwin K., Öpik, A. A. (Armin A., Australia. Bureau of Mineral Resources, G., & Geophysics. (1961). Lawn Hill, 4-mile geological series: Sheet E/54-9, Australian National Grid. Canberra : Dept. of National Development, Bureau of Mineral Resources, Geology and Geophysics.

Chakhmouradian, A.R., Mumin, A.H., Demény, A., Elliott, B., 2008. Postorogenic carbonatites at Eden Lake, Trans-Hudson Orogen (northern Manitoba, Canada): Geological setting, mineralogy and geochemistry. Lithos 103 (3), 503–526. https://doi.org/10.1016/j.lithos.2007.11.004.

Derrick, G. M. (1980). Australia 1:100 000 geological series. Sheet 6956 [Erl.]: Marraba: Queensland Commentary. Austral. Gov. Publ. Serv.

Downes, P.J., Demény, A., Czuppon, G., Jaques, A.L., Verrall, M., Sweetapple, M., Adams, D., McNaughton, N.J., Gwalani, L.G., Griffin, B.J., 2014. Stable H–C–O isotope and trace element geochemistry of the Cummins Range Carbonatite Complex, Kimberley region, Western Australia: implications for hydrothermal REE mineralisation, carbonatite evolution and mantle source regions. Miner. Deposita 49 (8), 905–932. https://doi.org/10.1007/s00126-014-0552-1.

Durand, C., Baumgartner, L.P., Marquer, D., 2015. Low melting temperature for calcite at 1000 bars on the join CaCO3-H2O – some geological implications. Terra Nova 27 (5), 364–369. https://doi.org/10.1111/ter.12168.

Ellis, D.J., Wyborn, L.A.I, 1984. Petrology and geochemistry of Proterozoic dolerites from the Mount Isa inlier. Record 9 (1), 19–32.

Etheridge, M.A., Rutland, R.W.R., Wyborn, L.A.I., 1987. Orogenesis and tectonic process in the early to middle proterozoic of northern australia. American Geophysical Union (AGU), pp. 131–147. https://doi.org/10.1029/GD017p0131.

Ferrero, S., Wunder, B., Ziemann, M.A., Wälle, M., O'Brien, P.J., 2016. Carbonatitic and granitic melts produced under conditions of primary immiscibility during anatexis in the lower crust. Earth Planet. Sci. Lett. 454, 121–131. https://doi.org/10.1016/j.epsl.2016.08.043.

Floess, D., Baumgartner, L.P., Vonlanthen, P., 2015. An observational and thermodynamic investigation of carbonate partial melting. Earth Planet. Sci. Lett. 409, 147–156. https://doi.org/10.1016/j.epsl.2014.10.031.

Foster, D.R.W., Austin, J., 2008. The 1800–1610Ma stratigraphic and magmatic history of the Eastern Succession, Mount Isa Inlier, and correlations with adjacent Paleoproterozoic terranes. Precambr. Res. 163 (1–2), 7–30. https://doi.org/10.1016/j.precamres.2007.08.010.

Foster, D.R.W., Rubenach, M.J., 2006. Isograd pattern and regional low-pressure, high-temperature metamorphism of pelitic, mafic and calc-silicate rocks along an east – west section through the Mt Isa Inlier. Aust. J. Earth Sci. 53 (1), 167–186. https://doi.org/10.1080/08120090500434617.

GBM Resources. (2012). Milo Scoping Study Announcement [ASX Announcement]. https://www.asx.com.au/asxpdf/20121122/pdf/42bcqm8hhz8ypk.pdf.

Geological Survey of Queensland. (2011). North-West Queensland Mineral and Energy Province report. [Brisbane] : Geological Survey of Queensland. https://trove.nla.gov.au/version/93308448.

Geological Survey of Queensland, Young, L. J., Lane, R. P., Withnall, I. W., Parsons, A., Pascoe, G. S., Turner, S. M., & Geoscience Australia. (2015). Marraba, Queensland [Map].
Gervasoni, F., Klemme, S., Rohrbach, A., Grützner, T., Berndt, J., 2017. Experimental constraints on the stability of baddeleyite and zircon in carbonate-and silicate-carbonate melts. Am. Mineral. 102 (4), 860–866.
Gibson, G.M., Champion, D.C., Withnall, I.W., Neumann, N.L., Hutton, L.J., 2018. Assembly and breakup of the Nuna supercontinent: Geodynamic constraints from 1800 to 1600 Ma sedimentary basins and basaltic magmatism in northern Australia. Precambr. Res. 313, 148–169. https://doi.org/10.1016/j.precamres.2018.05.013.
Giles, D., Betts, P., Lister, G., 2002. Far-field continental backarc setting for the 1.80–1.67 Ga basins of northeastern Australia. Geology 30 (9), 823–826. https://doi.org/10.1130/0091-7613(2002)030<0823:FFCBSF>2.0.CO;2.
Giles, D., Nutman, A.P., 2002. SHRIMP U–Pb monazite dating of 1600–1580 Ma amphibolite facies metamorphism in the southeastern Mt Isa Block. Australia. Australian Journal of Earth Sciences 49 (3), 455–465. https://doi.org/10.1046/j.1440-0952.2002.00931.x.
Goldstein, S.L., O'Nions, R.K., Hamilton, P.J., 1984. A Sm-Nd isotopic study of atmospheric dusts and particulates from major river systems. Earth Planet. Sci. Lett. 70 (2), 221–236. https://doi.org/10.1016/0012-821X(84)90007-4.
Hand, M., McLaren, S., Rubatto, D., 2002. The scale of the thermal problem in the Mount Isa Inlier. Geological Society of Australia Abstracts 67, 173.
Hill, E. J., Loosveld, R. J. H., & Page, R. W. (1992). Structure and Geochronology of the Tommy Creek Block, Mount Isa Inlier. In D. H. Blake & A. J. Stewart (Eds.), Detailed studies of the Mount Isa Inlier / A.J. Stewart & D.H. Blake, editors (pp. 329–348). Australian Govt. Pub. Service.
Hingst, R., 2002. Geology and geochemisry of the Cloncurry Fault, North-west Queensland. James Cook University, Australia.
Hoggard, M.J., Czarnota, K., Richards, F.D., Huston, D.L., Jaques, A.L., Ghelichkhan, S., 2020. Global distribution of sediment-hosted metals controlled by craton edge stability. Nat. Geosci. 13 (7), 504–510. https://doi.org/10.1038/s41561-020-0593-2.
Hoskin, P.W.O., 2005. Trace-element composition of hydrothermal zircon and the alteration of Hadean zircon from the Jack Hills, Australia. Geochim. Cosmochim. Acta 69 (3), 637–648. https://doi.org/10.1016/j.gca.2004.07.006.
Hoskin, P.W.O., Ireland, T.R., 2000. Rare earth element chemistry of zircon and its use as a provenance indicator. Geology 28 (7), 627–630. https://doi.org/10.1130/0091-7613(2000)28<627:REECOZ>2.0.CO;2.
Humphreys-Williams, E., Zahirovic, S., 2021. Carbonatites and global tectonics. Elements 17, 339–344. https://doi.org/10.2138/gselements.17.5.339.
Jell, P.A., 2013. Geology of queensland / edited by peter a jell. Geological Survey of Queensland Brisbane, Queensland.
Jochum, K.P., Weis, U., Stoll, B., Kuzmin, D., Yang, Q., Raczek, I., Jacob, D.E., Stracke, A., Birbaum, K., Frick, D.A., Günther, D., Enzweiler, J., 2011. Determination of reference values for NIST SRM 610-617 glasses following ISO guidelines. Geostand. Geoanal. Res. 35 (4), 397–429. https://doi.org/10.1111/j.1751-908X.2011.00120.x.
Keller, J., Hoefs, J., 1995. Stable isotope characteristics of recent natrocarbonatites from oldoinyo lengai. In: Bell, K., Keller, J. (Eds.), Carbonatite Volcanism, Vol. 4. Springer, Berlin Heidelberg, pp. 113–123. https://doi.org/10.1007/978-3-642-79182-6_9.
Lally, J., 1997. The structural history of the central Eastern Fold Belt, Mount Isa Inlier, Noerthwest Queensland, Australia [PhD Thesis]. James Cook University.
Le Maitre, R., Streckeisen, A., Zanettin, B., Le Bas, M., Bonin, B., & Bateman, P. (2002). Igneous Rocks: A Classification and Glossary of Terms. Igneous Rocks: A Classification and Glossary of Terms, Edited by R. W. Le Maitre and A. Streckeisen and B. Zanettin and M. J. Le Bas and B. Bonin and P. Bateman, Pp. 252. ISBN 0521619483. Cambridge, UK: Cambridge University Press, January 2005., 1.
Lee, W.-J., Fanelli, M.F., Cava, N., Wyllie, P.J., 2000. Calciocarbonatite and magnesiocarbonatite rocks and magmas represented in the system CaO-MgO-CO_2-H_2O at 0.2 GPa. Mineral. Petrol. 68 (4), 225–256. https://doi.org/10.1007/s007100050011.
Li, X.C., Zhou, M.F., Li, S.H., Zhang, X.R., Fan, H.R., Groves, D.I., Xuan Dac, N., 2023. An unusual early Eocene, syncollisional carbonatite complex and related rare earth element deposit in the India-Asia collision zone, northwestern Vietnam. Econ. Geol. 118 (1), 237–256.
Li, J., Ding, X., Liu, J., 2022. The role of fluids in melting the continental crust and generating granitoids: an overview. Geosciences 12 (8), 285.
Li, Z., Anenburg, M., Wei, C.W., Yuan, N., Xu, C., 2024. Carbonatite metasomatism in a subvolcanic setting: breccia at the Badou carbonatite in the North China Craton and implications for magmatic evolution and eruptive style. J. Petrol. 65 (7), egae069.
Liu, Y., Berner, Z., Massonne, H.-J., Zhong, D., 2006. Carbonatite-like dykes from the eastern Himalayan syntaxis: geochemical, isotopic, and petrogenetic evidence for melting of metasedimentary carbonate rocks within the orogenic crust. J. Asian Earth Sci. 26 (1), 105–120. https://doi.org/10.1016/j.jseaes.2004.10.003.
Loosveld, R.J.H., 1989. The intra-cratonic evolution of the central eastern Mount Isa Inlier, northwest Queensland. Australia. Precambrian Research 44 (3), 243–276. https://doi.org/10.1016/0301-9268(89)90047-8.
Loosveld, R.J.H., Etheridge, M.A., 1990. A model for low-pressure facies metamorphism during crustal thickening. J. Metam. Geol. 8 (3), 257–267. https://doi.org/10.1111/j.1525-1314.1990.tb00472.x.
Maas, R., McCulloch, M.T., Campbell, I.H., Page, R.W., 1987. Sm-Nd isotope systematics in uranium rare-earth element mineralization at the Mary Kathleen uranium mine. Queensland. Economic Geology 82 (7), 1805–1826. https://doi.org/10.2113/gsecongeo.82.7.1805.
Marshall, L. (2003). Brecciation within the Mary Kathleen Group of the Eastern Succession, Mt Isa Block, Australia: Implications of district-scale structural and metasomatic processes for Fe-oxide-Cu-Au mineralisation [Phd, James Cook University]. https://researchonline.jcu.edu.au/8243/.
Marshall, L., Oliver, N.H.S., Davidson, G.J., 2006. Carbon and oxygen isotope constraints on fluid sources and fluid–wallrock interaction in regional alteration and iron-oxide–copper–gold mineralisation, eastern Mt Isa Block. Australia. Mineralium Deposita 41 (5), 429–452. https://doi.org/10.1007/s00126-006-0069-3.
McDonough, W.F., Sun, S.-s., 1995. The composition of the Earth. Chem. Geol. 120 (3), 223–253. https://doi.org/10.1016/0009-2541(94)00140-4.
McLaren, S., Sandiford, M., Hand, M., 1999. High radiogenic heat–producing granites and metamorphism—An example from the western Mount Isa inlier. Australia. Geology 27 (8), 679–682. https://doi.org/10.1130/0091-7613(1999)027<0679:HRHPGA>2.3.CO;2.
Meeuws, F.J., Foden, J.D., Holford, S.P., Forster, M.A., 2019. Geochemical constraints on Cenozoic intraplate magmatism and their relation to Jurassic dolerites in Tasmania, using Sr-Nd-Pb isotopes. Chem. Geol. 506, 225–273.
Mitchell, R., 2005. Carbonatites and carbonatites and carbonatites. Can. Mineral. 43, 2049–2068. https://doi.org/10.2113/gscanmin.43.6.2049.
Nedosekova, I.L., Belyatsky, B.V., Belousova, E.A., 2016. Trace elements and Hf isotope composition as indicators of zircon genesis due to the evolution of alkaline-carbonatite magmatic system (Ilmeny–Vishnevogorsky complex, Urals, Russia). Russ. Geol. Geophys. 57 (6), 891–906. https://doi.org/10.1016/j.rgg.2015.09.021.
Oliver, N.H.S., Butera, K., Rubenach, M.J., Marshall, L., Cleverley, J., Mark, G., Tullemans, F., Esser, D., 2008. The protracted hydrothermal evolution of the Mount Isa Eastern Succession: a review and tectonic implications. Precambr. Res. 163 (1–2), 108–130. https://doi.org/10.1016/j.precamres.2007.08.019.
Oliver, N.H.S., Cartwright, I., Wall, V.J., Golding, S.D., 1993. The stable isotope signature of kilometre-scale fracturedominated metamorphic fluid pathways, Mary Kathleen. Australia. Journal of Metamorphic Geology 11 (5), 705–720. https://doi.org/10.1111/j.1525-1314.1993.tb00182.x.
Oliver, N.H.S., Holcombe, R.J., Hill, E.J., Pearson, P.J., 1991. Tectono-metamorphic evolution of the Mary Kathleen fold belt, northwest Queensland: a reflection of mantle plume processes? Aust. J. Earth Sci. 38 (4), 425–455. https://doi.org/10.1080/08120099108727982.
Oliver, N.H.S., Mark, G., Cleverley, J., Pollard, P., Rubenach, M., Marshall, L., Bastrakov, E., Williams, P., Nemchin, A., Baker, T., 2004. Modeling the role of sodic alteration in the genesis of iron oxide-copper-gold deposits, eastern mount isa block, Australia. Econ. Geol. 99, 1145–1176. https://doi.org/10.2113/gsecongeo.99.6.1145.
Özkan, M., Çelik, Ö.F., Marzoli, A., Çörtük, R.M., Billor, M.Z., 2021. The origin of carbonatites from the eastern Armutlu Peninsula (NW Turkey). J. Geol. Soc. London 178 (6), jgs2020-171. https://doi.org/10.1144/jgs2020-171.
Palmer, D.A.S., Williams-Jones, A.E., 1996. Genesis of the carbonatite-hosted fluorite deposit at Amba Dongar, India; evidence from fluid inclusions, stability isotopes, and whole rock-mineral geochemistry. Econ. Geol. 91 (5), 934–950. https://doi.org/10.2113/gsecongeo.91.5.934.
Paton, C., Hellstrom, J., Paul, B., Woodhead, J., Hergt, J., 2011. Iolite: Freeware for the visualisation and processing of mass spectrometric data. J. Anal. at. Spectrom 26 (12), 2508–2518. https://doi.org/10.1039/C1JA10172B.
Pourteau, A., Smit, M.A., Li, Z.-X., Collins, W.J., Nordsvan, A.R., Volante, S., Li, J., 2018. 1.6 Ga crustal thickening along the final Nuna suture. Geology 46 (11), 959–962. https://doi.org/10.1130/G45198.1.
Rubenach, M.J., 1992. Proterozoic low-pressure/high-temperature metamorphism and an anticlockwise P–T–t path for the Hazeldene area, Mount Isa Inlier, Queensland. Australia. Journal of Metamorphic Geology 10 (3), 333–346. https://doi.org/10.1111/j.1525-1314.1992.tb00088.x.
Rubenach, M.J., Barker, A.J., 1998. Metamorphic and metasomatic evolution of the Snake Creek Anticline, Eastern Succession, Mt Isa Inlier. Aust. J. Earth Sci. 45 (3), 363–372. https://doi.org/10.1080/08120099808728397.
Rubenach, M.J., Foster, D., Evins, P., Blake, K., Fanning, C., 2008. Age constraints on the tectonothermal evolution of the Selwyn Zone, Eastern Fold Belt. Mount Isa Inlier. Precambrian Research 163 (1–2), 81–107. https://doi.org/10.1016/j.precamres.2007.08.014.
Sandiford, M., Eraser, G., Arnold, J., Foden, J., Farrow, T., 1995. Some causes and consequences of high-temperature, low-pressure metamorphism in the eastern Mt Lofty Ranges, South Australia. Aust. J. Earth Sci. 42 (3), 233–240. https://doi.org/10.1080/08120099508728197.
Sandiford, M., Hand, M., McLaren, S., 1998. High geothermal gradient metamorphism during thermal subsidence. Earth Planet. Sci. Lett. 163 (1), 149–165. https://doi.org/10.1016/S0012-821X(98)00183-6.
Schmidt, M.W., Giuliani, A., Poli, S., 2024. The origin of carbonatites—combining the rock record with available experimental constraints. J. Petrol. 65 (10). https://doi.org/10.1093/petrology/egae105.
Schumann, D., Martin, R.F., Fuchs, S., de Fourestier, J., 2019. Silicocarbonatitic melt inclusions in fluorapatite from the Yates prospect, Otter Lake, Québec: evidence of marble anatexis in the central metasedimentary belt of the Grenville Province. Can. Mineral. 57 (5), 583–604. https://doi.org/10.3749/canmin.1900015.
Simandl, G.J., Paradis, S., 2018. Carbonatites: Related ore deposits, resources, footprint, and exploration methods. Appl. Earth Sci. 127 (4), 123–152. https://doi.org/10.1080/25726838.2018.1516935.
Simonetti, A., Bell, K., 1994. Nd, Pb and Sr isotopic data from the Napak carbonatite-nephelinite centre, eastern Uganda: An example of open-system crystal fractionation. Contrib. Miner. Petrol. 115 (3), 356–366. https://doi.org/10.1007/BF00310774.

Simonetti, A., Bell, K., Viladkar, S.G., 1995. Isotopic data from the Amba Dongar Carbonatite Complex, west-central India: evidence for an enriched mantle source. Chem. Geol. 122 (1), 185–198. https://doi.org/10.1016/0009-2541(95)00004-6.

Slezak, P., Spandler, C., 2020. Petrogenesis of the gifford creek carbonatite complex, Western Australia. Contrib. Miner. Petrol. 175. https://doi.org/10.1007/s00410-020-1666-3.

Slezak, P., Spandler, C., Border, A., Whittock, K., 2021. Geology and ore genesis of the carbonatite-associated Yangibana REE district, Gascoyne Province. Western Australia. Mineralium Deposita 56 (5), 1007–1026. https://doi.org/10.1007/s00126-020-01026-z.

Southgate, P.N., Bradshaw, B.E., Domagala, J., Jackson, M.J., Idnurm, M., Krassay, A.A., Page, R.W., Sami, T.T., Scott, D.L., Lindsay, J.F., McConachie, B.A., Tarlowski, C., 2000. Chronostratigraphic basin framework for Palaeoproterozoic rocks (1730–1575 Ma) in northern Australia and implications for base-metal mineralisation. Aust. J. Earth Sci. 47 (3), 461–483. https://doi.org/10.1046/j.1440-0952.2000.00787.x.

Stepanov, A.S., Aminov, J., Odinaev, S., Iskandarov, F.S., Jiang, S.-Y., Karmanov, N.S., 2024. Fluoritites produced by crystallization of carbonate–fluoride magma. J. Petrol. 65 (4). https://doi.org/10.1093/petrology/egae033.

Tanaka, T., Togashi, S., Kamioka, H., Amakawa, H., Kagami, H., Hamamoto, T., Yuhara, M., Orihashi, Y., Yoneda, S., Shimizu, H., Kunimaru, T., Takahashi, K., Yanagi, T., Nakano, T., Fujimaki, H., Shinjo, R., Asahara, Y., Tanimizu, M., Dragusanu, C., 2000. JNdi-1: a neodymium isotopic reference in consistency with LaJolla neodymium. Chem. Geol. 168 (3), 279–281. https://doi.org/10.1016/S0009-2541(00)00198-4.

Taylor, H.P., Frechen, J., Degens, E.T., 1967. Oxygen and carbon isotope studies of carbonatites from the Laacher See District, West Germany and the Alnö District. Sweden. Geochimica et Cosmochimica Acta 31 (3), 407–430. https://doi.org/10.1016/0016-7037(67)90051-8.

Tichomirowa, M., Grosche, G., Gotze, J., Belyatsky, B., Savva, E., Keller, J., Todt, W., 2006. The mineral isotope composition of two Precambrian carbonatite complexes from the Kola Alkaline Province – Alteration versus primary magmatic signatures. Lithos 91 (1–4), 229–249. https://doi.org/10.1016/j.lithos.2006.03.019.

Tilton, G.R., Bryce, J.G., Mateen, A., 1998. Pb–Sr–Nd Isotope Data from 30 and 300 Ma collision zone carbonatites in northwest pakistan. J. Petrol. 39 (11–12), 1865–1874. https://doi.org/10.1093/petroj/39.11-12.1865.

Tshiningayamwe, M., Bolhar, R., Nex, P.A.M., 2022. A zircon trace element and Hf isotope geochemical study of syenites and carbonatite, exemplified by the Epembe alkaline carbonatite complex. Namibia. South African Journal of Geology 125 (3–4), 307–322. https://doi.org/10.25131/sajg.125.0021.

Wen, J., Bell, K., Blenkinsop, J., 1987. Nd and Sr isotope systematics of the Oka complex, Quebec, and their bearing on the evolution of the sub-continental upper mantle. Contrib. Miner. Petrol. 97 (4), 433–437. https://doi.org/10.1007/BF00375321.

Wickramasinghe, W.A.G.K., Madugalla, T.B.N.S., Athurupana, B., Zhao, L., Zhai, M., Li, X., Pitawala, H.M.T.G.A., 2024. An unusual occurrence of carbonatites derived from the crust in the UHT granulite facies metamorphic terrain of Sri Lanka. Precambr. Res. 410, 107502. https://doi.org/10.1016/j.precamres.2024.107502.

Williams-Jones, A.E., Vasyukova, O.V., Kostyuk, A.V., 2024. Niobium ore genesis in a capsule. Geology 52 (7), 560–564. https://doi.org/10.1130/G52169.1.

Wilson, I.H., 1978. Volcanism on a Proterozoic continental margin in northwestern Queensland. Precambr. Res. 7 (3), 205–235. https://doi.org/10.1016/0301-9268(78)90039-6.

Witt, W.K., Hammond, D.P., Hughes, M., 2019. Geology of the Ngualla carbonatite complex, Tanzania, and origin of the Weathered Bastnaesite Zone REE ore. Ore Geol. Rev. 105, 28–54. https://doi.org/10.1016/j.oregeorev.2018.12.002.

Woolley, A., Bailey, D., 2012. The crucial role of lithospheric structure in the generation and release of carbonatites: geological evidence. Mineral. Mag. 76. https://doi.org/10.1180/minmag.2012.076.2.02.

Woolley, A. R., & Kempe, D. R. C. (1989). Carbonatites: Nomenclature, average chemical compositions, and element distribution. https://api.semanticscholar.org/CorpusID:100384517.

Wu, H., Zhu, W., Ge, R., 2022. Evidence for carbonatite derived from the earth's crust: The late Paleoproterozoic carbonate-rich magmatic rocks in the southeast Tarim Craton, northwest China. Precambr. Res. 369, 106425. https://doi.org/10.1016/j.precamres.2021.106425.

Wyborn, L., 1998. Younger ca 1500 Ma granites of the Williams and Naraku Batholiths, Cloncurry district, eastern Mt Isa Inlier: Geochemistry, origin, metallogenic significance and exploration indicators. Aust. J. Earth Sci. 45 (3), 397–411. https://doi.org/10.1080/08120099808728400.

Wyborn, L., Page, R., Mcculloch, M., 1988. Petrology, geochronology and isotope geochemistry of the post-1820 Ma granites of the Mount Isa Inlier: mechanisms for the generation of Proterozoic anorogenic granites. Precambr. Res. 40–41, 509–541. https://doi.org/10.1016/0301-9268(88)90083-6.

Wyllie, P.J., Tuttle, O.F., 1960. The system CaO–CO2–H2O and the origin of carbonatites1. J. Petrol. 1 (1), 1–46. https://doi.org/10.1093/petrology/1.1.1.

Yaxley, G.M., Anenburg, M., Tappe, S., Decree, S., Guzmics, T., 2022. Carbonatites: classification, sources, evolution, and emplacement. Annu. Rev. Earth Planet. Sci. 50 (1), 261–293. https://doi.org/10.1146/annurev-earth-032320-104243.

Yuhara, M., Hirahara, Y., Nishi, N., Kagami, H., 2005. Rb-Sr, Sm-Nd ages of the phalaborwa carbonatite complex, South Africa. Polar Geoscience 18, 101–113.